Food Hydrocolloids 162 (2025) 111004

Contents lists available at ScienceDirect

Food Hydrocolloids

journal homepage: www.elsevier.com/locate/foodhyd

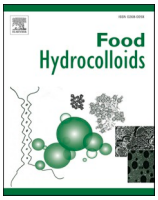

Starch-tannin interactions: Influence of grape tannins on structure, texture, and digestibility of starches from different botanical sources

Harkamal Kaur [a], Annu Mehta [b], Lokesh Kumar [a,*]

[a] Department of Wine, Food and Molecular Biosciences, Lincoln University, Lincoln 7647, New Zealand
[b] Food Experience and Sensory Testing Laboratory, Massey University, Palmerston North, New Zealand

ARTICLE INFO

Keywords:
Botanical sources
Grape seed tannins
Grape skin tannins
In-vitro digestion
Rheology
Starch

ABSTRACT

This study investigated the effect of grape seed (GSd) and grape skin (GSk) tannins on the physicochemical, rheological properties and in-vitro digestibility of starches (corn, pea and wheat) derived from three different botanical sources. Quantification of bound and unbound tannins using MCP and HPLC analysis demonstrated that majority of the tannins were bound to starch molecules. The results of particle size distribution, starch-iodine binding and FTIR studies indicated the development of inclusion complexes through hydrophobic interactions with tannins in pea starch, while other two starches prominently formed non-inclusion complexes via hydrogen bonding. Back extrusion analysis of textural properties indicated that wheat starch-tannin complexes resulted in firmer starch-tannin gels compared to other two starches. Rheological studies revealed an increase in the viscoelastic modulus (G' and G") with improved elastic behavior for all starch-tannin gels. Starches complexed with tannins demonstrated strong antioxidant properties and in-vitro starch digestion studies revealed significant reductions in rapidly digestible starch (RDS) and slowly digestible starch (SDS), along with an increase in resistant starch (RS), particularly in pea starch complexed with GSd tannins. This study enhanced our understanding of how GSd and GSk tannins influence the properties of starches from various botanical origins, helping in understanding starch-tannin interactions and enabling the creation of foods with improved texture and digestibility.

1. Introduction

Carbohydrates, fats and proteins are the three major biomacromolecules abundantly present in the staple foods. Among carbohydrates, majority of the dietary calorie intake is contributed by starch (D. Amoako & J. M. Awika, 2016; Mohamed, 2023). This plant-based essential biopolymer, generally stored in the form of starch granules either water soluble glycogen or water insoluble particles, is the prime storage carbohydrate on this planet (Apriyanto et al., 2022). Glucose units, linked through two types of glycosidic linkages (α-1, 4 and α-1, 6), form the molecular structure of this versatile biomaterial (Apriyanto et al., 2022; Compart et al., 2023). The physicochemical-cum-sensory properties of starch-based foods are largely defined by the interplay between the structural features of starch, including its crystallinity type, granule structure, glycosidic linkage, and the synergistic assembly of its linear (amylose) and branched (amylopectin) glucose chains, which vary depending on the botanical source (Mohamed, 2023; Obadi & Xu, 2021). Gelatinized or retrograded forms of starch are generally included in foods; moreover texture and flavour enhancement of the cooked starch is hugely dependent on the cooking procedure and the presence-cum-interaction of other biomolecules (phenolic compounds, lipids, proteins and salts) with starch. Starch is categorized as a digestible food macromolecule which gets digested in small intestine. However, its rapid digestion can lead to quick spikes in blood glucose levels, which may increase the risk of developing metabolic disorders such as obesity and diabetes (Mohamed, 2023; Takahama & Hirota, 2018).

Grapes, a rich source of diverse polyphenols (e.g., gallic acid, ellagic acid, epicatechins, catechins, epigallocatechin gallate, gallocatechin, procyanidins, anthocyanidins and resveratrol), are recognized for their excellent antioxidant, anti-inflammatory and anti-carcinogenic properties. The polyphenols/flavonoids such as catechins, epicatechins and procyanidins along with other compounds like gallic acid, epicatechin gallate and epigallocatechin gallate particularly in grape seeds and skins, influence the properties of starch-based food matrices by modifying starch retrogradation, digestibility, and glycemic responses significantly (Sochorova et al., 2020; Wang et al., 2022; Watrelot &

* Corresponding author.
E-mail address: lokesh.kumar@lincoln.ac.nz (L. Kumar).

https://doi.org/10.1016/j.foodhyd.2024.111004
Received 11 October 2024; Received in revised form 6 December 2024; Accepted 18 December 2024
Available online 27 December 2024

Norton, 2020; Zhang et al., 2020).

Condensed tannins, also referred as proanthocyanidins, are prominent in grape-derived products and act as plant "defenders" due to their involvement in the cellular functioning and plant bioactivities like scavenging of free radicals and reactive oxygen species (D. Amoako & J. M. Awika, 2016; Watrelot & Norton, 2020). These tannins, composed of flavan-3-ols like catechins and epicatechins, containing phenolic hydroxyl group, constitute the basic subunit in these non-hydrolysable tannins (Barrett et al., 2018; Ngo et al., 2022) and can alter the food properties by interacting with various bio-macromolecules present in food systems through covalent and non-covalent bonding. These molecules exhibiting antioxidant nature can potentially aid in improving health by elevating the nutritional profile of food products (D. Amoako & J. M. Awika, 2016; Takahama & Hirota, 2018). Polyphenols also influence the fluidity, hardness, viscosity and other rheological properties of starches (Wu et al., 2024; Zhu, 2015). Various studies have observed alterations in the flow behavior index and viscoelastic behavior of starch gels upon tannin addition (Wu et al., 2024), reporting an increase in the viscoelastic modulus of starch gels with enhanced elastic behavior (Kan et al., 2022; Xu et al., 2021). Moreover, grape seed and skin tannins enhance the organoleptic properties of foods by imparting pigmentation and astringent flavour (Kennedy et al., 2001), while their interactions with carbohydrates can effectively control the glucose release in alimentary canal (Barrett et al., 2018). Together, these properties position grape-derived tannins as multifunctional agents capable of improving both the functional and nutritional attributes of starch-based food systems.

Molecular interaction between starch and tannins occurs through non-covalent bonding, i.e. hydrogen bonding, electrostatic, hydrophobic and ionic interactions, which can lead to the formation of inclusion and non-inclusion complexes of tannin and starch (particularly V-type inclusion and non V-type complexes) (Takahama & Hirota, 2018; Wang et al., 2023; Xu et al., 2021). Several structural studies, such as FTIR, have revealed the interaction of tannins with starch through non-covalent bonds, with the absence of new peaks indicating the formation of complexes without significant structural changes (Luo et al., 2024; Youming et al., 2024; Zhang et al., 2023).

In V-type inclusion complexes, the hydrophobic effect of water favours the wrapping of starch around the monomeric tannin molecules in a spiral manner, forming a strong molecular association between the two biomolecules with improved crystalline order. In contrast, loose non-V type complexes involve molecular interactions between starch and tannins primarily through hydrogen bonding, without significant changes in the order of crystallinity of starch due to steric hindrances. These interactions act as connectors between starch chains, leading to aggregation without altering the crystalline structure (Wang et al., 2023; Wu et al., 2024; Xu et al., 2021).

Alterations in the physicochemical-cum-nutritional properties of starch, such as digestibility, gelatinization, gelling, order of crystallinity, pasting properties, retrogradation, rheology, structure and thermal behavior, occur after the addition of non-hydrolysable tannins during food processing (Zhu, 2015). These changes are attributed to the monomeric and polymeric nature of tannins (Ngo et al., 2022; Wang et al., 2023; Xu et al., 2021), as well as the development of a network structure within starch-tannin gels driven by non-covalent interactions (Wu et al., 2024; Zhu, 2015). Glycan chain length and amylopectin to amylose ratio in starch, and molecular size plus number of hydroxyl groups in tannins largely define the complexation between these two molecules. Apart from it, processing methods also affect the binding between tannin and starch. Complexation can be carried out using physical, chemical and enzymatic methods. During gelatinization, leached off amylose can effectively bind with the tannins and changes in the molecular arrangement of glycan chains can occur, leading to an improved integration between these two biomolecules (Ngo et al., 2022; Wang et al., 2023; Xu et al., 2021).

Complexation of starch with tannins produces resistant starch, which can contribute to human well-being and can potentially alleviate the intensity of chronic diseases as tannins avert the rejoining of glycan chains and as a result affecting the properties of starch along with in vivo controlled release of glucose in intestines. Investigations have been carried out to assess the factors responsible behind starch-tannin interactions and the positive health benefits furnished by these respective complexes through regulation of glycemic response (Hernández et al., 2022; Ngo et al., 2022; Rostamabadi et al., 2023). However, most studies have focused on examining the effects of individual tannins, such as gallic acid (Gutierrez et al., 2020), epicatechin/epigallocatechin gallate (Luo et al., 2024) and other polyphenolic compounds (Kan et al., 2022; Li et al., 2023; Liu et al., 2023; Luo et al., 2024; Wei et al., 2019; Youming et al., 2024; Zhang et al., 2023; Zhang et al., 2020), on various starches at different tannin concentrations.

While hydrophobic and hydrophilic interactions are key factors in the formation of starch-tannin complexes, particularly for starches with varying amylose content, to our knowledge, no study has specifically investigated the influence of botanical origin of starch on these complex formations. This study aims to examine the impact of botanical origin of starch, along with external factors such as presence of grape seed and skin tannins, their properties (e.g. degree of polymerization and monomeric/polymeric content), and storage conditions, on starch properties after complex formation. The goal is to better understand the molecular interactions underlying inclusion and non-inclusion complex formation between polymeric grape seed (GSd) tannins and monomeric/oligomeric grape skin (GSk) tannins and starches derived from different botanical sources (corn, pea and wheat) through particle size distribution, FT-IR, and starch-iodine binding experiments, and their effect on modifying the textural-cum-rheological properties of starch, as well as their significant impact on starch digestibility. These findings could provide insights into the distinct binding patterns of tannins with starches as well as into the molecular interactions that contribute to the development of functional foods with refined textures and potential health benefits, particularly minimizing postprandial glucose release, thereby improving both food quality and human health.

2. Materials and methods

2.1. Materials

The grape seed (GSd) tannins (Enartis Tan UVA) used in this study were high molecular weight condensed tannins extracted from grape seeds with 78% purity (w/w according to methyl cellulose precipitate (MCP) analysis). The grape skin (GSk) tannins derived from grape skins (ViniTannin™ SR, 2 B FermControl) with 81% purity (w/w determined through MCP analysis) were rich in gallic acid and other mono/oligomeric tannins. Ethanol, methanol, HCl, methyl cellulose, ammonium sulphate, potassium iodide, iodine, sodium acetate, ethyl acetate, acetic acid, iron chloride, 2, 4, 6 - Tris (2 –pyridyl) – S - triazine (TPTZ), ascorbic acid, phloroglucinol, and sodium hydroxide (NaOH) were used to perform different analysis. The chemicals of analytical grade were obtained from Sigma - Aldrich and were used in the experiments without further modifications. Three different types of starch derived from different botanical sources, i.e. corn starch (amylose content – 26 %), pea starch (amylose content – 31.01 %) and wheat starch (amylose content – 30 %), were used to conduct the experiments. The amylose content of these three starches was determined using the enzymatic assay kit (Amylose/Amylopectin Assay Kit, Megazyme International Ireland Ltd., Wicklow, Ireland). Pea starch (Xin Liang) and corn starch (Pams) were obtained from New Zealand's local suppliers and wheat starch was obtained from Sigma - Aldrich. De-ionized water was used in all of the experiments.

2.2. Preparation of heat treated starch-tannin complexes

Starch was dissolved at a concentration of 5% (w/v) in deionized

water. Grape seed (GSd) and skin (GSk) tannins at a concentration of 0.5% (w/v of the mixture) in de-ionized water were added to the starch solution to prepare starch-tannin complexes. Prior to cooking the starch-tannin complexes, GSd and GSk tannins were hand stirred for 2 min in de-ionized water followed by magnetic stirring for the next 10 min at 2000 rpm under room temperature conditions. This mixture was used for MCP and mDP analysis. To the dissolved tannin solution, starch was added and the final volume was made up to hundred milliliter. The concentration of starch was kept constant in all samples. Both control and starch-tannin mixtures were cooked in water bath (95 °C) for 30 min with constant stirring (200 rpm). To maintain consistent conditions and minimize water loss during the preparation of starch-tannin complexes, the starch samples were covered, and the water bath was sealed with a fitted cover throughout the 30-min heating process at 95 °C. Following that, freshly prepared control samples and starch-tannin complexes were analyzed for quantification of bound and unbound tannins, starch-iodine complex formation, particle size distribution, textural and rheological characterizations. The freeze dried samples were used for other characterizations. Additionally, to investigate the de-polymerization of tannins under thermal treatment via HPLC studies, 0.5% (w/v of the mixture) grape tannin mixture, dissolved in de-ionized water, was magnetically stirred at 95 °C for 30 min, followed by freeze drying.

2.3. Characterization of tannins

2.3.1. Methyl cellulose precipitate (MCP) assay

The freshly prepared tannin sample solution (section 2.2) was centrifuged for 5 min at 10,000 rpm at 20 °C and the obtained supernatant was transferred to fresh micro-centrifuge tube and used for MCP and mean degree of polymerization (mDP) analysis.

For MCP, 100 μL of the tannin sample (diluted to 1/10 concentration) was poured in a clean micro-centrifuge tube and 300 μL methyl cellulose reagent (0.04%) was added in the treatment samples. The reaction between the two components was allowed to take place by incubating the samples for 2 min. In case of control samples, no methyl cellulose was added. Then, 200 μL of ammonium sulphate was added in both control and treatment samples. The final volume was adjusted to 1000 μL by the addition de-ionized water followed by incubation of the samples for 10 min. The incubated samples were centrifuged at 10,000 rpm for 5 min. UV–Vis spectroscopy (UV-1800, SHIMADZU) of the supernatant was carried out 280 nm. The standard curve was derived by plotting the absorbance (280 nm) against the concentration of epicatechins (0–120 mg/L). The tannin content in the final solution was calculated using the formula as follows (Smith, 2015):

A_{280} due to tannin = A_{280} Control - A_{280} Supernatant

Epicatechin in final solution (μg/mL) = (A_{280} due to tannin – Intercept) / Slope

Epicatechin in the extract (μg/mL) = Epicatechin in final solution / (Sample volume / 1000)*Dilution rate

2.3.2. mDP

The mean degree of polymerization (mDP) of tannins derived from grape skin and grape seed extracts was determined by the method proposed by (Kennedy & Jones, 2001). Based on the MCP tannin concentration, sample volume to be loaded into the cartridge was kept at around 10 mg of tannin, ensuring maximum recovery and preventing breakthrough (performed in duplicates). Prior to sample loading, activation of the C18 cartridge (500 mg SEP-PAK cartridge, WAT043395, Global Science, Auckland, New Zealand) was carried out by adding 7.5 mL of each of the three different solvents in the following order: methanol, ethyl acetate and deionized water. The samples (4 mL, 10 mg concentration) were loaded into the cartridge, followed by washing with deionized water (5 mL) and then dried using the nitrogen gas for 60–90 min with the flow rate of 1 L per minute. Once the cartridges were dried, the monomeric phenols were washed off by passing ethyl acetate (5 mL) through the cartridge. While, the polymeric fraction was collected using methanol (5 mL) followed by rotary evaporation at 40 °C and resuspension in one mL of methanol. The re-suspended polymeric tannin solution was kept at −20 °C until further analysis.

To perform phloroglucinolysis, the phloroglucinol reagent was prepared in a 20 mL volumetric flask. Solution 1 [ascorbic acid (0.4 g) suspended in methanol (8 mL) containing 36% HCl (0.35 mL)] and solution 2 [phloroglucinol (2 g) dissolved in 8 mL methanol] were combined together and the final volume was adjusted to 20 mL using methanol. The freshly prepared phloroglucinol reagent (0.5 mL) was mixed with an equal volume of the above prepared polymeric tannin solution in a Kimax tube and gently vortexed. The reaction mixture was allowed to react for 20 min at 50 °C in a water bath. The reaction was stopped by adding sodium acetate solution (5 mL, 40 mM) to the reaction mixture. After vortexing, the solution was transferred into an HPLC vial following filtration through a PTFE syringe filter with a pore size of 0.45 μm and a diameter of 13 mm.

The cleaved polyphenolic products (assayed in duplicates) were identified and qualified using an Agilent series HPLC machine (Waldbronn, Germany). The calculations for catechin equivalent molar response areas were determined according to the method outlined by (Kennedy & Jones, 2001). Quantification of the polyphenolic cleavage products was achieved using a catechin calibration curve. Based on the molarity of the compounds, the percent relative molar compositions of phloroglucinol adducts (extension subunits) and flavan-3-ol monomers (terminal subunits) were determined. The mDP and conversion yield (%) were calculated using the following formula:

$$\text{mDP} = \frac{\text{Sum of all terminal and extension subunits (in moles)}}{\text{Sum of all terminal subunits (in moles)}}$$

$$\text{Conversion yield}(\%) = \frac{\text{Epicatechin equivalent total tannin concentration (obtained from phloroglucinolysis)}}{\text{Epicatechin equivalent total tannin concentration (measured from MCP tannin assay)}}$$

2.3.3. HPLC

Freeze dried samples (0.2 g) of tannins and starch-tannin complexes were suspended in absolute methanol (10 mL) and magnetic stirred for 30 min followed by centrifugation at 10,000 rpm for 5 min at 22 °C. The collected supernatant was syringe filtered through a membrane (0.45 μm) and 10 μL of it was injected into HPLC column (Ace® 5 column, 250 × 4.6 mm, Advanced Chromatography Technologies, Aberdeen, Scotland) to determine the phenolic concentration of respective samples. Following the initiation of separation, chromatograms were captured at 280 nm using a photodiode array detector for compound identification and quantification. Furthermore, the corresponding chromatogram of duplicate samples underwent scanning from 220 nm to 600 nm using fluorescence detectors. The analysis was conducted in duplicates for all

samples.

2.4. Quantification of bound and unbound tannins

The quantification of bound and unbound tannins was carried out using an MCP analysis (section 2.3.1). Prior to performing MCP, freshly prepared starch control samples and starch-tannin complexes were kept at room temperature to alleviate the temperature of cooked samples and were then centrifuged for 5 min at 10,000 rpm at 20 °C. The supernatant, containing unbound tannins, was transferred to fresh micro-centrifuge tube and MCP analysis was carried out. The amount of bound and unbound tannins in starch-tannin complexes was calculated using the following equation:

Bound tannins = Initial tannins – Unbound tannins

Where,

Bound tannins = Tannins complexed with starch.

Initial tannins = Amount of tannins complexed with starch (0.5 g, 10% of dry weight of starch).

Unbound tannins = Tannins released in the supernatant.

2.5. Starch-iodine binding

Binding of iodine with starch and starch-tannin complexes was analyzed using UV–Vis spectrophotometer (UV-1800, SHIMADZU). Both thermally treated control and tannin treated starch samples were diluted 200 times prior to the addition of iodine. Iodine solution was prepared by mixing 1.5 g of potassium iodide in approximately 12.5 mL of de-ionized water followed by dissolving iodine (0.635 g) to it, followed by final volume made up to 50 mL. Light exposure of the freshly prepared iodine solution was avoided to prevent the decomposition of iodine. To analyze the influence of tannins in starch-tannin complexes, absorption spectra (900 - 500 nm) was recorded by transferring test samples (0.9 mL) and iodine solution (0.1 mL) to the cuvette (Liu et al., 2023).

2.6. Particle size distribution

Mastersizer 3000 (Malvern Panalytical, UK) was used to measure the particle size of the freshly prepared control samples and starch-tannin complexes with constant absorption index (0.01) and refractive index (1.53). For stabilizing the size distribution, flushing of the machine with pure de-ionized water was carried out. The obscuration limits (10%) for measurement were met by diluting the respective samples in deionized water (400 mL) and the accuracy of the system was ensured by dispersing the samples using an automated system (Chen et al., 2021). Once the obscuration limits were reached, the particle size distribution, Dx10, Dx50, Dx90 and volume-weighted mean diameter (D [4,3]) of the samples were measured by the instrument.

2.7. FTIR

The spectrophotometric analysis of starch and its complexes was identified using Thermo Scientific™ Nicolet™ iS™5 FT-IR spectrometer equipped with Bacchus 3 Multispec analyzer. One mg of finely grounded freeze dried tannin samples and starch-tannin complexes were mixed with 100 mg of KBr. The mixture was compressed into thin layers and the spectrum was scanned for 64 times within the absorbance range of 400–4000 cm^{-1} with resolution of 4 cm^{-1} under room temperature conditions. The background adjustments (prior to each measurement) and the corrections of acquired spectra using the function “atmospheric compensation”, were made through the built-in OPUS software (Version 7.2).

2.8. Textural properties

The back extrusion textural analysis of the heat treated control samples and starch-tannin gels, stored at 4 °C overnight, was carried out using TA-XT2i Texture Analyzer (Stable Micro Systems Ltd, Surrey, UK). A five kg load cell, compression disc and back-extrusion cell (A/BE-d35 RIG) were used. The compression cycle set up for the experiment involved test speed of 1 mm/s for 30 mm distance and post-test speed of 10 mm/s. Different extrusion parameters, i.e. cohesiveness, consistency, firmness and index of viscosity, were measured and recorded by an in-built software (Exponent (Version 6,2,4,0), Stable Micro Systems Ltd, Surrey, UK). Firmness is defined as the deformation of material under applied pressure and is measured as a maximum force recorded before deformation of the material. Consistency, ability of the material to maintain its shape, is deduced from the positive area upon compression and thicker consistency of the sample is demonstrated by the higher consistency value. Cohesiveness, measures the stickiness of a substance, is defined by the negative force upon the return back of the disc. The index of viscosity, a measure of resistance of a fluid flow, is defined as the area under back extrusion. The viscosity index is calculated from the area under the peak negative force in a force – time graph.

2.9. Rheological measurements of starch-tannin complexes

Prior to measuring the rheological properties using an MCR 302 Rheometer (Anton Paar, Graz, Austria) equipped with cone plate of diameter: 49.953 mm and cone angle (°) of 0.986 positioning length (mm), the freshly prepared starch tannin gels were allowed to cool down for 90 min to reach room temperature. Amplitude sweep tests were conducted to measure the storage modulus (G′) and loss modulus (G″) as a function of strain, covering a range from 0.001 to 1.00%. These tests identified 1% strain as being within the linear viscoelastic region. Subsequently, frequency sweep tests were performed at this constant strain over an angular frequency range of 1–100 rad/s at room temperature. The storage modulus and loss modulus derived from frequency sweep data were fitted by applying power law model as shown below:

$$\sigma = K.\ \gamma^{n},$$

Where,

σ = shear stress (Pa), K = consistency coefficient ($Pa.s^n$), γ = shear rate (s^{-1}) and n = flow behavior index (n = 1 represents Newtonian fluid, and n < 1 represents pseudo-plastic behavior).

2.10. Antioxidant assays

Antioxidant capability of starch-tannin complexes through ferric reduction was determined by using ferric reducing antioxidant power (FRAP) (Wu et al., 2021) and ABTS (2,2′-azinobis (3-ethyl-benzothiazoline-6-sulfonic acid) reagent solutions (Esfandi et al., 2019; Re et al., 1999).

2.10.1. FRAP assay

One gram of freeze dried control and treatment samples were suspended in 70% methanol (20 mL) and subjected to overnight stirring. The following day, suspended samples were centrifuged for 10 min at 2500 rpm and the supernatant was collected to perform the FRAP assay. In Greiner 96 U-Bottom plate, control and treatment samples (250 μL) were mixed with 2.5 mL of freshly prepared FRAP reagent, which was made by dissolving acetate buffer (0.3 mM, pH 3.6), TPTZ (10 mM) in HCl (40 mM) and $FeCl_3$ together in the ratio of 10:1:1. Absorbance of the reaction mixture was immediately measured at 593 nm using FLUOstar Omega (BMG LABTECH) spectrophotometer. Then, incubation of the samples for 2 h at 37 °C was carried out followed by absorbance measurement at 593 nm. For the standard curve, $FeSO_4$ solution was used and the sample results were expressed as μmol Fe^{3+} per g sample (Wu

et al., 2021).

2.10.2. ABTS assay

The ABTS antioxidant assay was carried out using the methods described by (Esfandi et al., 2019; Re et al., 1999). The ABTS solution was prepared by combining 2.45 mM of potassium persulphate and 7 mM of ABTS stock solution in a 1:1 ratio, followed by an overnight magnetic stirring in the absence of light. To attain the absorbance range near 0.7 ± 0.02 at 734 nm, phosphate buffer saline (pH 7.4) was used to dilute the above-prepared ABTS solution. 200 μL of the diluted ABTS solution was mixed with 20 μL of the control starch and starch-tannin complexes in the Greiner 96 U-Bottom plate. Two absorbance measurements were taken at a wavelength of 734 nm: one immediately after mixing the sample with the ABTS reagent and the second absorbance, measured at the same wavelength, after incubating the reaction mixture at 37 °C for 6 min. For the standard curve, concentration of Trolox solution was plotted against the absorbance and the results for ABTS assay were expressed as mmol TE equivalents per g sample.

2.11. In-vitro starch digestibility

In-vitro starch digestibility assay of the freeze dried samples for determining rapidly digesting starch (RDS), slowly digesting starch (SDS) and resistant starch (RS) was performed using Digestible and Resistant Starch Assay Kit (Megazyme, Bray, Ireland). The digestion experiment was carried out as per the digestion kit protocol. Samples (0.5 g) were suspended in 0.5 mL of 95 % ethanol followed by addition of 17.5 mL of sodium maleate buffer (50 mM, pH 6.0, containing 2 mM $CaCl_2$). To equilibrate the temperature to 37 °C, the solutions were magnetic stirred for 5 min. Once the desired temperature was attained, enzyme suspension (1 mL) and sodium maleate buffer (1.5 mL, 50 mM, pH 6.0, containing 2 mM $CaCl_2$) were added and the reaction mixture was stirred continuously. The enzyme suspension was prepared by adding 2.5 g of pancreatic alpha amylase and amyloglucosidase (PAA/AMG), to cold distilled water (35 mL), followed by 5 min magnetic stirring in the fume hood. Then, 17 g of ammonium sulphate suspended in 50 mL of distilled water was added to it and stored at 4 °C. After 20 min, 1 mL of the solution was taken out from the reaction mixture to determine the rapidly digesting starch (RDS). Acetic acid solution (20 mL, 50 mM) was added to it to stop the reaction. Further, 2 mL of the solution was transferred to fresh micro-centrifuge tube and centrifuged for 5 min at 13,000 rpm and the supernatant was collected. Aliquots of collected supernatant (in triplicates) were transferred to 15 mL falcon tube and 1 mL of amyloglucosidase (AMG) solution (solution 2 used as such as provided in the kit) was added. The samples were mixed and incubated for 30 min at 50 °C. Then, GOPOD reagent (3 mL) was added to the samples and re-incubated for another 20 min. The absorbance of the samples was measured at 510 nm using UV–Vis spectrophotometer (UV-1800, SHIMADZU). To determine slowly digesting starch (SDS), the samples were taken after 120 min and the same protocol was repeated as for the RDS. The standard solutions were prepared by mixing 1 mL of constituents provided in bottle 5 (D-glucose, 1 mg/mL) with 0.1 mL of sodium acetate buffer (100 mM, pH 4.5) and 3.0 mL of GOPOD reagent. The blank reagents were prepared by adding sodium acetate buffer (0.2 mL, 100 mM, pH 4.5) into 3.0 mL of GOPOD reagent.

To determine resistant starch (RS), after 240 min of magnetic stirring at 37 °C, 4 mL of the solution was transferred into a 15 mL falcon tube and 95 % ethanol (4 mL) was added to it. The samples were centrifuged at 4000 rpm for 10 min and the supernatant was discarded. The pellet was re-suspended in 50 % ethanol (2 mL), vortexed and then, 6 mL of ethanol (50 %) was added followed by centrifugation at 4000 rpm for 10 min. This step of pellet suspension in ethanol was repeated twice. Then, the samples were put in ice/water bath and magnetic bead was added to the pellet and cold solution of NaOH (2 mL, 1.7 M) was added to re-suspend the pellets. After 20 min of magnetic stirring, 8 mL of sodium acetate buffer (1 mM) and 0.1 mL of AMG solution were added to the samples and incubated at 50 °C for 30 min with intermittent mixing using a vortex. Two milliliters of the sample solution was transferred to fresh micro-centrifuge tubes and centrifuged at 13,000 rpm for 5 min and supernatant was collected. To 0.1 mL of the aliquot, 0.1 mL of sodium acetate buffer (100 mM) and 3 mL of GOPOD reagent were added followed by incubation at 50 °C for 20 min. The absorbance was measured at 510 nm using UV–Vis spectrophotometer (UV-1800, SHIMADZU).

2.12. Statistical analysis

The experiments were conducted in triplicates unless specifically mentioned and the data was presented as means ± SD. Analysis of results was carried out using One - way ANOVA and Tukey's comparison (statistical significance determined using $p < 0.05$ for the entire study). Minitab® 21.3.1 software was employed to run the statistical analysis. The figures and fitting of models was carried out using OriginPro 2024 (SR1 10.1.0.178). Figs. 1, 4J and 6 and 7D and 8 were created in BioRender.

3. Results & discussion

3.1. Characterization of tannins

The tannin content for GSd and GSk tannins, quantified through MCP, varied significantly (Table 1), which was 3915.29 ± 80.62 epicatechin eq. mg/L and 4147.55 ± 37.53 epicatechin eq. mg/L, respectively, suggesting that the tannin content in GSk was higher compared to GSd. Fig. 2A presents the HPLC chromatogram of GSd and GSk tannins monitored at 280 nm and their respective concentrations (mg/L) are presented in Table 1. Peaks for various monomeric tannins were identified by their relative retention times. Peaks marked from 1 to 7 in Fig. 2A represent monomeric tannins, assigned as gallic acid, procyanidin B1, catechin, procyanidin B2, epicatechin, epigallocatechin gallate and epicatechin gallate, respectively. The monomeric tannin content in GSk was higher (mainly gallic acid and epicatechin gallate content) than that in GSd, however, for GSd, a broad peak was observed between 58 and 72 min at 280 nm (Fig. 2B), well separated from the monomeric peaks, indicating the presence of condensed polymeric material. In case of GSk, no polymeric fraction hump was present, suggesting that the majority of the phenolics present in the sample are in monomeric and/or oligomeric form. Further, the detailed differences in the phenolic profiles were analyzed through mDP. The relative proportions of constitutive subunits in tannins were significantly unique (Fig. 2C). In both tannins, catechin was the most abundant terminal subunit and epicatechin exhibited the highest proportion as the extension subunit. Epicatechin gallate as both the extension and terminal subunit was also observed. Epigallocatechin was also detected as an extension subunit in addition to the other three subunits. In both GSd and GSk, the terminal subunits comprised 47–50% catechin, 36–38% epicatechin and 11–15% epicatechin gallate. The extension subunit composition for the two tannins ranged between 74 and 76% for epicatechin, 9–11% for catechin and epicatechin gallate and lower than 3% for epigallocatechin. The mDP of grape tannins was quite low, with GSd of 6.3 and GSk of 5.6, showing no significant differences. The conversion yield (%) for GSd was significantly greater (69%) than that of GSk (19%) (Table 1). Consequently, the higher conversion yield in GSd, as indicated by its mDP along with the detection of a polymeric hump through HPLC studies, could be associated with the presence of condensed tannins in higher proportions. In contrast, the lower recovery yield in GSk could be likely due to the presence of the majority of the tannins in the mono/oligomeric forms, as revealed by mDP and HPLC. Additionally, HPLC analysis confirmed that GSk contains a larger amount of monomeric/oligomeric tannins than GSd.

Previous research has primarily focused on grape seed tannins, specifically dimers and oligomeric procyanidins, and their effects on

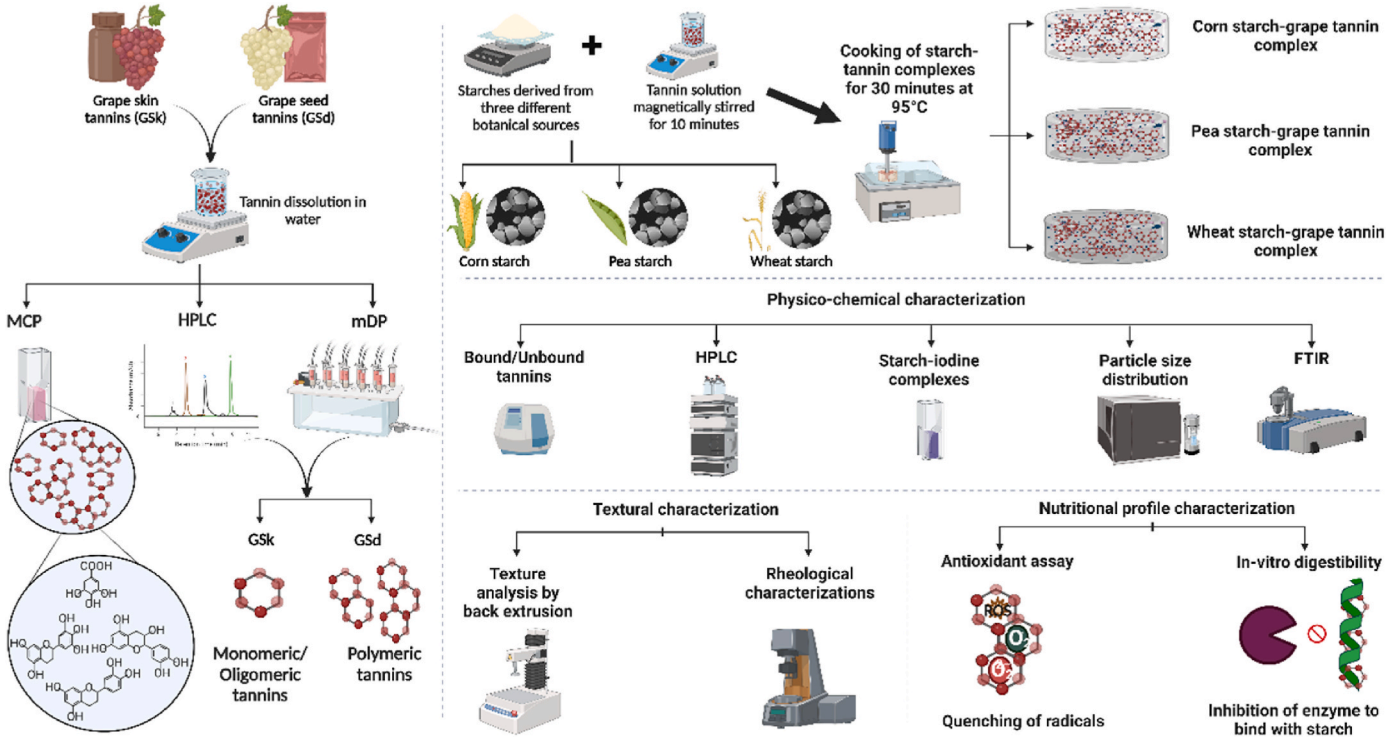

Fig. 1. Experimental scheme of the study.

starch properties, including antioxidant activity and digestibility (Sochorova et al., 2020; Wang et al., 2022; Watrelot & Norton, 2020; Zhang et al., 2020). Some studies have compared grape seed polyphenols with those from other botanical sources (Wang et al., 2021) or examined the effects of grape skin phytonutrients on starch-digesting enzymes (Miao et al., 2014). However, most of these investigations lack detailed exploration of the polyphenolic profile of the used tannins and its interaction with starch. Presence of procyanidins in the grape skin tannins makes its polyphenolic profile unique, as these are not commonly found in other tannin-rich plant sources like persimmon and sorghum. Furthermore, studies on tannins from other sources, such as sorghum and persimmon (D. B. Amoako & J. M. Awika, 2016; Barros et al., 2012; Du et al., 2019; Li et al., 2018; Mkandawire et al., 2013), have largely been limited to starches of the same botanical origin and variations in amylose content, leaving the role of tannin composition and molecular mechanisms underexplored. Persimmon tannins are mainly a mixture of phenolic compounds and high molecular weight condensed tannins, which exhibit greater absorbability, making it difficult to clearly define the persimmon tannin profile. As a result, crude persimmon plant peels/pulps/extracts are often used, which majorly contain catechins, epicatechin, ferulic acid, flavonoids, gallic acid, p-coumaric acid and condensed tannins (Butt et al., 2015; Gu et al., 2008). In contrast sorghum tannins primarily consist of ferulic acid and protocatechuic acid, with smaller amounts of gallic acid, cinnamic acid, p-coumaric acid, vanillic acid, p-hydroxybenzoic acid, syringic acid, and caffeic acid (de Morais Cardoso et al., 2017). The tannin profiles for these polyphenols vary significantly from one source to another, and the unique composition of grape tannins offers new insights to study starch-tannin interactions. Our grape seed and skin tannins were found to be rich in gallic acid, catechins, epicatechins, epicatechin gallate, epigallocatechin gallate and procyanidins B1 and B2, along with the polymeric condensed tannins in grape seed tannins. This diverse profile could form the basis for understanding the interactions between grape tannins and starch at a molecular level and understand how grape skin and seed tannins bind to starch, as a result impacting the starch structure, texture and digestibility.

3.2. Quantification of bound and unbound tannins

MCP results clearly showed that the three different starches complexed with both GSd and GSk tannins had higher amounts of bound tannins (for GSd ≥3830 epicatechin eq. mg/L and for GSk >4100 epicatechin eq. mg/L) along with lower levels of unbound tannins (Table 2). This indicates an efficient interaction (~98–99%) between tannins and starch following thermal treatment. Youming et al., (2024) observed an increase in the amount of tannins bound to the corn starch following complexation at elevated temperatures, accompanied by higher tannin concentrations. Our findings are also consistent with the studies conducted by Kan et al. (2022), who reported a significant increase in the tannin content bound to starch after complexation with wheat starch. The binding of tannins with starch is strongly influenced by the source and structure of starch, the type of tannin compound and the cooking method used (Wu et al., 2024). Cooking of starch at or above its gelatinization temperatures for longer periods allows for pore development and structural disintegration of starch granules, along with providing sufficient time for the development of molecular interactions between starch molecules and other biomolecules, such as tannins, present in the matrix (Barros et al., 2012; Kan et al., 2022). It is possible that smaller sized monomeric tannins entered inside the granules via the pores and complexed with the glycan chains, while highly condensed tannins got trapped within the pores during starch gelatinization, resulting in them being detected in lesser amounts as unbound tannins (D. B. Amoako & J. M. Awika, 2016; Ribeiro de Barros, 2012). Moreover, the phenomenon of gelatinization transition and embedding of tannins within the amorphous hydrophobic areas of amylose helices is highly dependent on the botanical source of starch, which further influences starch interactions with tannins at a molecular level (Donmez et al., 2021; Ribeiro de Barros, 2012; Wu et al., 2024).

3.2.1. HPLC analysis of extractable tannins

To further elucidate the precise interactions between tannins and starch in starch-tannin complexes, and to quantify the amount of extractable or loosely bound tannins to starch, HPLC analysis of starch-

Table 1
Differences in tannin profiles of grape seed (GSd) and grape skin (GSk) tannins.

	MCP (epicatechin eq. mg/L)	mDP	Conversion yield (w/w %)	HPLC (phenolic concentration, mg/L)							
				Gallic acid	Procyanidin B1	Catechin	Procyanidin B2	Epicatechin	Epigallocatechin gallate	Epicatechin gallate
GSd	3915.29 ± 80.62^{b}	6.29 ± 0.13^{a}	69.00 ± 0.02^{a}	32.45 ± 0.47^{b}	242.46 ± 0.99^{a}	443.70 ± 1.26^{a}	264.50 ± 0.62^{a}	269.16 ± 1.26^{b}	25.57 ± 0.38^{b}	19.49 ± 1.25^{b}
GSk	4147.55 ± 37.53^{a}	5.62 ± 0.27^{a}	19.00 ± 0.02^{b}	192.12 ± 1.91^{a}	113.22 ± 1.52^{b}	432.04 ± 1.41^{b}	126.96 ± 1.63^{b}	294.57 ± 1.43^{a}	43.35 ± 0.44^{a}	132.07 ± 1.73^{a}

Statistical differences between different tannin samples were assessed using One - way ANOVA ($P < 0.05$), data presented as mean ± standard deviation, different letters indicate significant differences between GSd and GSk tannins, conversion yield was calculated as follows: (Epicatechin equivalent total tannin concentration (obtained from phloroglucinolysis))/(Epicatechin equivalent total tannin concentration (measured from MCP tannin assay)).

tannin complexes was carried out. The results discussed in section 3.1 showed that the concentration of solutions containing only tannins was significantly higher for both highly condensed GSd and mono/oligomeric GSk. However, addition of starch to the tannin solution followed by thermal treatment significantly reduced the levels of GSd (condensed tannins) and GSk (mono/oligomeric tannins) to almost undetectable levels in all starch-tannin complexes, suggesting that most of the tannins interacted with starch (Table 3 and Fig. 3A). Our results are in accordance with Barros et al. (2012), who also found a significant reduction in both mono/oligomeric and condensed tannin content after cooking various starches with sorghum phenolic tannins. They suggested that a decline in the mono/oligomeric tannins in the starch-tannin complexes indicates that these types of tannins were predominantly involved in the interactions with starch.

Moreover, HPLC studies investigating heat-induced de-polymerization of tannins revealed the breakdown of polymeric tannins into their monomeric subunits. As shown in Fig. 3B, a shift in the peaks of polymeric materials confirms the degradation of polymeric tannins. mDP analysis identified catechins and epicatechins as the prominent terminal and extension subunits. The HPLC data (Table 3) indicated an increase in phenolic concentration after heat treatment, particularly for catechins and epicatechins in GSd tannins, which increased from 443.70 ± 1.26 to 524.44 ± 8.69 for catechins and from 269.16 ± 1.26 to 341.99 ± 9.62 for epicatechins. These findings are consistent with observations that thermal treatment de-polymerizes polymeric tannins into monomeric forms, leading to an increase in the concentration of these subunits (Salazar-Orbea et al., 2021).

Additionally, Barros et al. (2012) noted a decrease in the peak of polymeric tannins after thermal treatment for 30 min, attributing the change to heat induced de-polymerization. In the case of starch-GSd tannin complexes, the complete disappearance of the polymeric peaks may be due to the entrapment of polymeric tannins within the surface pores formed by the rupturing of starch granules under elevated temperature, coupled with the development of stronger hydrogen bonds with starch, thus making these tannins "unextractable" in contrast to the smaller monomeric tannins (Barros et al., 2012; Prommajak et al., 2020). MCP studies further quantified bound and unbound tannins, revealing that 98–99% of tannins were bound to starch, with only 1–2% remaining extractable. Given such low concentrations, it is possible that the polymeric hump may not be detectable. The reduction of mono/-oligomeric tannins to undetectable levels in starch-tannins complexes along with the absence of a polymeric peak suggests that tannins have likely interacted significantly with starch, possibly through hydrogen bonding or hydrophobic interactions (Barros et al., 2012).

3.3. *Particle size distribution*

The two parameters, i.e. particle size and size distribution, are crucial to determine the tannin interactions and their effect on starch structural properties. All three starches and their complexes with tannins exhibited bimodal particle distribution. In case of corn and wheat starch-tannin complexes, despite the conjugation between tannins and starch molecules, the particle sizes of starch remained unchanged. Meanwhile, the starch particle size was significantly affected upon addition of tannins into pea starch solutions. In case of corn starch control, wheat starch control and both starch–grape seed and grape skin tannin complexes, the particle size distribution peak was spread within the range of 20–100 μm. For pea starch control samples, the peak particle size was centered approximately over 20–200 μm range, while the peak for tannin and pea starch complexes was centered over a larger range, indicating that the complexation of starch with tannins increased the size of starch molecules and broadened the particle size peak within the range of 20–700 μm (Fig. 4A–C). Similarly, an increase in mean particle size of maize starch was observed by Liu and co-workers (2023) upon addition of polymeric proanthocyanidins. They concluded that the tannins either lead to the aggregation or expansion of starch granule

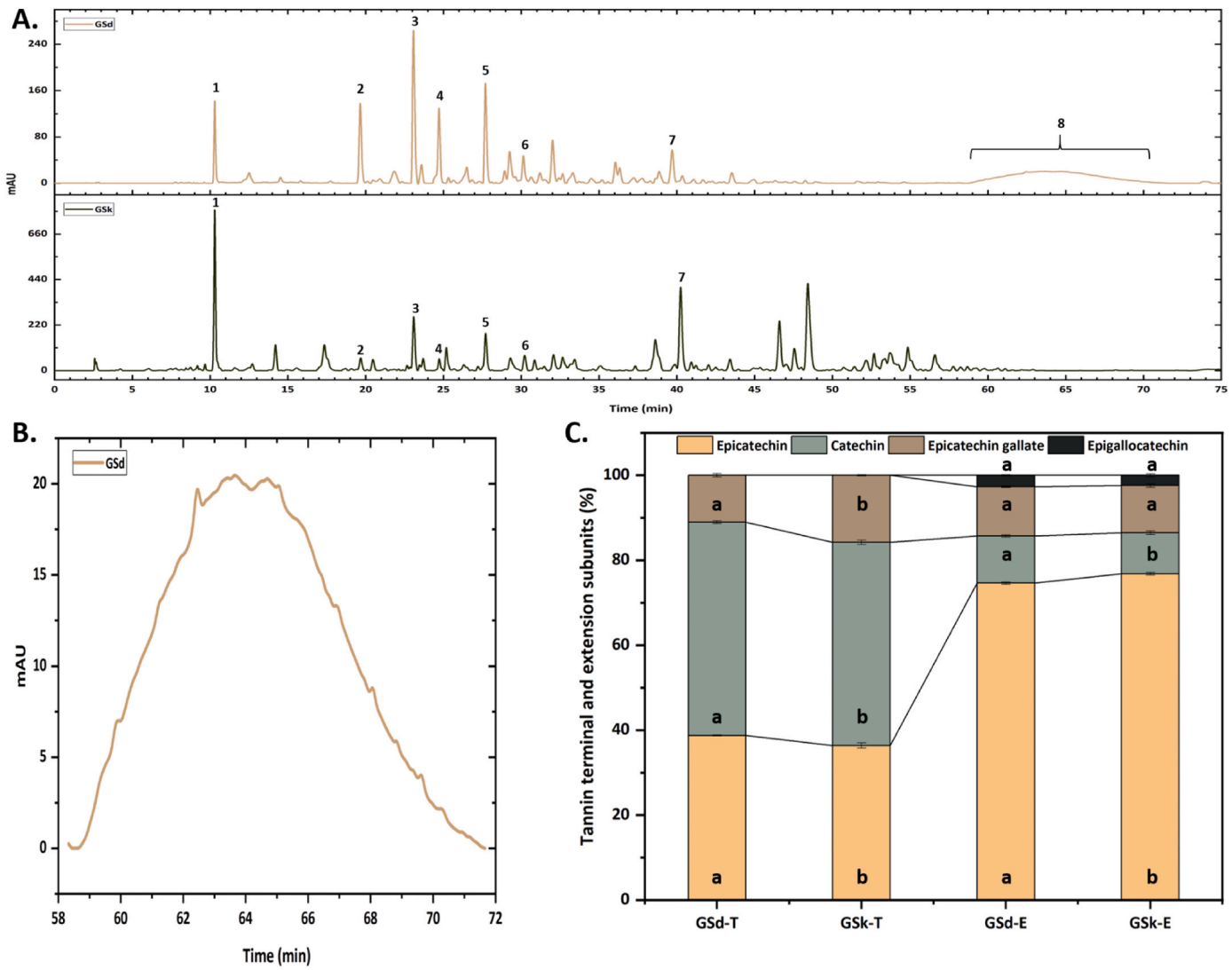

Fig. 2. (A) HPLC chromatograms of grape seed (GSd) and grape skin (GSk) tannins, [1. Gallic acid, 2. Procyanidin B1, 3. Catechin, 4. Procyanidin B2, 5. Epicatechin, 6. Epigallocatechin gallate, 7. Epicatechin gallate and 8. Polymeric hump], (B) Polymeric hump for GSd tannins at 280 nm and (C) Tannin composition of GSd and GSk analyzed through mDP, GSd-T: Grape seed terminal subunit, GSk-T Grape skin terminal subunit, GSd-E: Grape seed extension subunit, GSk-E Grape skin extension subunit. Statistically significant differences between the values of samples prior to incubation and after 4 h of incubation are represented by different alphabetical letters ($p < 0.05$).

particles upon interaction. It was further elaborated that the size of starch particles might have increased due to the embedding of tannin molecules into the helical cavities of amylose via hydrophobic interactions and formation of inclusion complexes (Liu et al., 2023). Luo et al. (2024) also suggested the incorporation of polyphenols into pea starch granules, along with their binding to starch chains and surfaces, may act as a bridge, facilitating the clustering of starch molecular chains. However, in case of other two starches, the particle size almost remained unchanged, suggesting that either the tannins could be incorporated between the two amylose helices, facilitating their connection through hydrophilic interactions (hydrogen bonding interactions and/or van der Waals forces), thus, causing minimal or no changes in the particle size of the starch (Liu et al., 2023) or the type of granules, crystalline type, amylose content and gelatinization properties of the starches might have contributed to the observed changes. This suggests that tannins alone may not account for the increase in particle size, instead, the inherent properties and aggregation behavior of starch granules from different botanical sources likely play a significant role, which could explain the unchanged particle size for these two starches (Bridson et al., 2019; Jane, 2004).

The volume-weighted diameter for the starch control and starch-tannin complexes varied significantly. Both pea starch-grape seed tannin (PGSd) and pea starch-grape skin tannin (PGSk) complexes exhibited higher D [4,3] values, which were greater than 150 μm, followed by pea starch control (68 μm). Corn starch, wheat starch and their respective complexes showed almost similar D [4,3] values. The Dx (10) values for starch control samples and its respective tannin complexes were significantly different from each other, which were higher for starch-grape skin tannin complexes, followed by starch–grape seed complexes and the starch control samples for all the three different starches. Similarly, the Dx (50) and Dx (90) significantly increased for pea and wheat starch–grape skin complexes followed by pea and wheat starch–grape seed complexes, except for corn starch–grape tannin complexes, which exhibited an opposite trend in contrast to other two starches and their respective starch-tannin complexes (Table 2). The findings are in agreement with those of Bridson et al. (2019), who also observed an increase in the D (50) and D (90) values for starches and proposed that this increase could be either from the encapsulation of starch granules with tannins or the clustering of the starch granules.

Table 2
Percent of tannins bound to starch in different starch-tannin complexes, particle size of starch control samples and starch-tannin complexes.

	Total tannins (Epicatechin eq. mg/L)	Unbound Tannins (Epicatechin eq. mg/L)	Bound Tannins (Epicatechin eq. mg/L)	Percent of Bound Tannins (%)	Dx (10)	Dx (50)	Dx (90)	D [4,3]
CSC*	–	–	–	–	25.17 ± 0.25^{c}	41.35 ± 0.42^{c}	63.72 ± 0.81^{c}	42.69 ± 0.49^{d}
CGSd	3915.29 ± 80.62^{b}	72.83 ± 2.31^{c}	3842.46 ± 5.00^{c}	98%	25.83 ± 0.10^{b}	42.38 ± 0.06^{a}	64.79 ± 0.13^{a}	43.44 ± 0.15^{d}
CGSk	4147.55 ± 37.53^{a}	38.87 ± 0.58^{d}	4108.68 ± 2.63^{b}	99%	26.20 ± 0.26^{a}	42.13 ± 0.17^{b}	64.12 ± 0.14^{b}	43.59 ± 0.07^{d}
PSC	–	–	–	–	27.73 ± 0.57^{c}	64.22 ± 2.43^{c}	114.90 ± 6.80^{c}	68.01 ± 3.15^{c}
PGSd	3915.29 ± 80.62^{b}	87.56 ± 1.16^{a}	3827.73 ± 0.83^{e}	98%	44.75 ± 1.31^{b}	135.75 ± 8.35^{b}	304.50 ± 13.97^{b}	199.75 ± 47.10^{a}
PGSk	4147.55 ± 37.53^{a}	42.14 ± 1.74^{d}	4105.41 ± 6.03^{b}	99%	50.82 ± 7.93^{a}	178.30 ± 48.80^{a}	383.20 ± 83.00^{a}	157.05 ± 7.45^{b}
WSC	–	–	–	–	11.00 ± 0.00^{c}	39.53 ± 0.06^{b}	66.75 ± 0.11^{b}	40.03 ± 0.06^{d}
WGSd	3915.29 ± 80.62^{b}	82.24 ± 2.89^{b}	3833.05 ± 2.63^{d}	98%	11.18 ± 0.04^{b}	38.83 ± 0.07^{c}	66.20 ± 0.14^{c}	45.81 ± 0.14^{d}
WGSk	4147.55 ± 37.53^{a}	24.14 ± 1.74^{e}	4123.41 ± 4.65^{a}	99%	16.90 ± 0.10^{a}	43.64 ± 0.13^{a}	76.84 ± 0.27^{a}	39.55 ± 0.08^{d}

Data presented as mean ± standard deviation, same letters indicate treatments are not significantly different ($p < 0.05$).
*CSC: Corn starch control, CGSd: Corn starch-grape seed tannin complex, CGSk: Corn starch-grape skin tannin complex, PSC: Pea starch control, PGSd: Pea starch-grape seed tannin complex, PGSk: Pea starch-grape skin tannin complex, WSC: Wheat starch control, WGSd: Wheat starch-grape seed tannin complex, WGSk: Wheat starch-grape skin tannin complex.

Table 3
Differences in extractable tannin profiles of different starch-tannin complexes.

	Gallic acid (mg/L)	Procyanidin B1 (mg/L)	Catechin (mg/L)	Procyanidin B2 (mg/L)	Epicatechin (mg/L)	Epigallocatechin gallate (mg/L)	Epicatechin gallate (mg/L)
GSd	32.45 ± 0.47^{d}	242.46 ± 0.99^{b}	443.70 ± 1.26^{b}	264.50 ± 0.62^{b}	269.16 ± 1.26^{d}	25.57 ± 0.38^{d}	19.49 ± 1.25^{d}
GSk	192.12 ± 1.91^{b}	113.22 ± 1.52^{c}	432.04 ± 1.41^{c}	126.96 ± 1.63^{d}	294.57 ± 1.43^{b}	43.35 ± 0.44^{c}	132.07 ± 1.73^{b}
GSd (heat treated)	43.08 ± 0.08^{c}	292.58 ± 4.39^{a}	524.44 ± 8.69^{a}	306.82 ± 4.55^{a}	341.99 ± 9.62^{a}	65.73 ± 8.55^{b}	44.37 ± 2.35^{c}
GSk (heat treated)	230.19 ± 0.16^{a}	108.71 ± 1.91^{d}	386.69 ± 3.20^{d}	132.30 ± 3.66^{c}	278.09 ± 5.42^{c}	80.71 ± 2.43^{a}	199.57 ± 1.75^{a}
CGSd	0.95 ± 0.03^{h}	1.58 ± 0.04^{f}	9.37 ± 0.37^{fg}	1.78 ± 0.24^{f}	5.18 ± 0.16^{f}	0.11 ± 0.02^{e}	0.13 ± 0.03^{e}
CGSk	7.31 ± 0.15^{g}	0.92 ± 0.01^{f}	5.20 ± 0.12^{g}	1.08 ± 0.02^{f}	3.78 ± 0.09^{f}	0.17 ± 0.01^{e}	0.23 ± 0.03^{e}
PGSd	2.55 ± 0.04^{h}	6.55 ± 0.14^{e}	22.89 ± 0.64^{e}	6.95 ± 0.22^{e}	14.82 ± 0.45^{e}	0.50 ± 0.02^{e}	0.37 ± 0.01^{e}
PGSk	13.07 ± 0.06^{f}	1.21 ± 0.01^{f}	13.47 ± 0.10^{f}	1.44 ± 0.14^{f}	8.55 ± 0.12^{ef}	0.32 ± 0.03^{e}	0.72 ± 0.03^{e}
WGSd	2.63 ± 0.10^{h}	2.41 ± 0.05^{f}	22.83 ± 0.22^{e}	2.92 ± 0.31^{ef}	13.83 ± 0.19^{e}	0.14 ± 0.02^{e}	0.30 ± 0.05^{e}
WGSk	16.54 ± 0.40^{e}	0.66 ± 0.01^{f}	12.75 ± 0.38^{f}	0.66 ± 0.11^{f}	8.35 ± 0.21^{ef}	0.18 ± 0.02^{e}	0.49 ± 0.02^{e}

(Data presented as mean ± standard deviation, same letters indicate treatments are not significantly different ($p < 0.05$).
GSd: Grape seed tannins, GSk: Grape skin tannins, CGSd: Corn starch-grape seed tannin complex, CGSk: Corn starch-grape skin tannin complex, PGSd: Pea starch-grape seed tannin complex, PGSk: Pea starch-grape skin tannin complex, WGSd: Wheat starch-grape seed tannin complex, WGSk: Wheat starch-grape skin tannin complex.

3.4. Starch-iodine binding

Iodine complexes with the hydroxyl (-OH) groups present at the exterior positions of the helical structure of amylose (Liu et al., 2023) and gets lodged into its hydrophobic spiral cavity after forming a linear polyiodide chain (Amoako & Awika, 2019). This amylose-iodine complex generates a coloured complex, with absorbance measured within the spectral range of 900–500 nm (Liu et al., 2023). Tannins can interact with amylose in two ways: either by integrating into the intra-helical structure and developing inclusion complexes, thereby making the spiral cavity inaccessible to iodine and reducing/inhibiting the formation of amylose-iodine complexes or incorporating into the inter-helical space due to limited hydrogen bonding between these two biomolecules, i.e. amylose and tannins. In the latter scenario, tannins form non-inclusion complexes, leaving the amylose cavity accessible to iodine, thus allowing the formation of amylose-iodine complex (Amoako & Awika, 2019).

For corn starch control (CSC) and their respective starch-tannin complexes, no shift in the absorbance values was observed. Meanwhile, for wheat starch-tannin complexes, a decrease in absorbance within the wavelength range of 500–650 nm was observed in contrast to the wheat starch control (WSC). Similarly, compared to the pea starch, which gave the absorbance maxima at 650 nm, the absorbance for pea starch-tannin complexes significantly reduced (Fig. 4G–I). Liu et al. (2023) reported similar results for wheat starch and polymeric proanthocyanidin complexes. The conjugation of proanthocyanidins with starch molecules hindered the complexation between iodine and starch molecules, which led to a decrease in the absorbance values. Amoako & Awika (2019) also observed a significant decrease in the absorbance values for starch–proanthocyanidin complexes as compared to the starch samples devoid

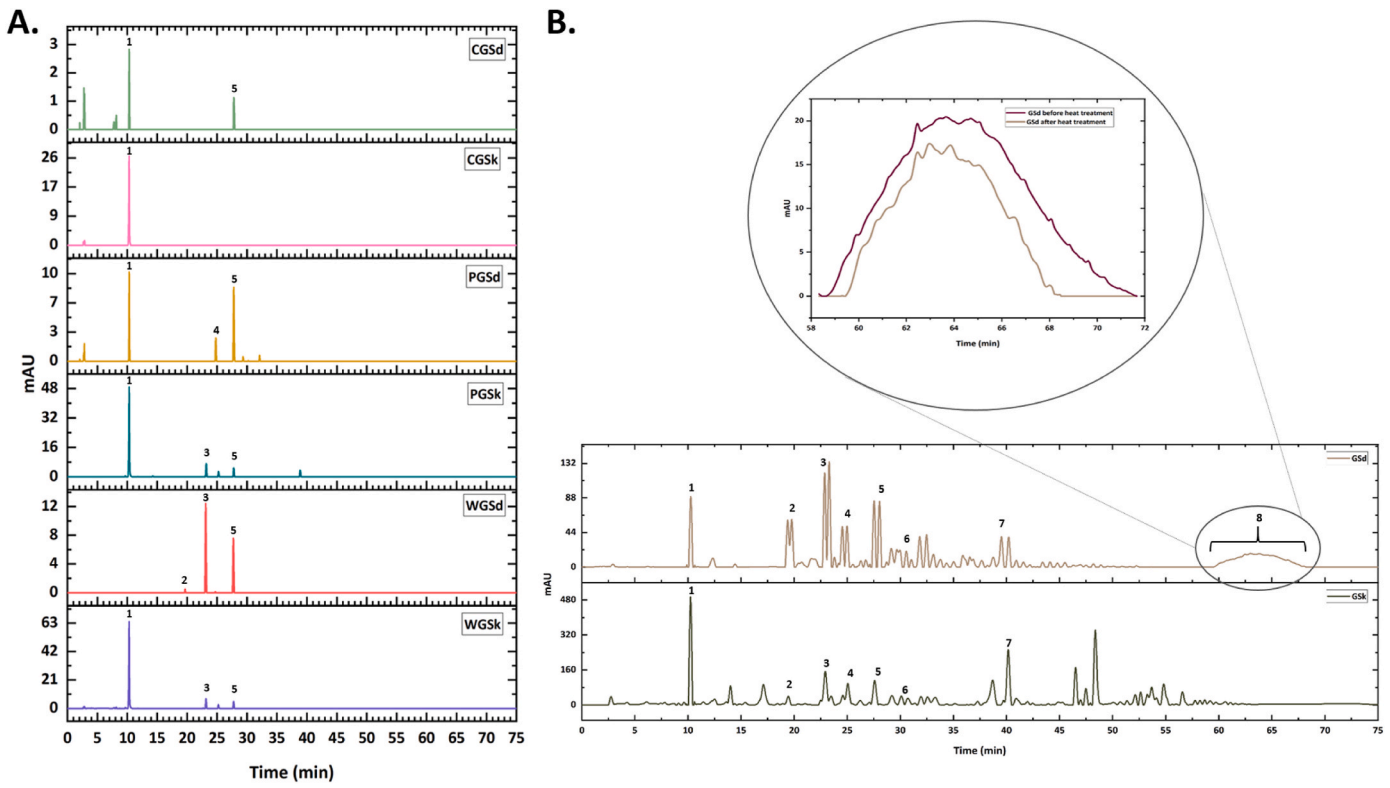

Fig. 3. HPLC chromatograms showing: (A.) the extractable or loosely bound grape tannin content in starch-tannin complexes, (B.) the thermally treated GSd and GSk tannins, illustrating a reduction in polymeric GSd tannin content due to the de-polymerization of polymeric GSd tannins after heat treatment. [1. Gallic acid, 2. Procyanidin B1, 3. Catechin, 4. Procyanidin B2, 5. Epicatechin, 6. Epigallocatechin gallate, 7. Epicatechin gallate and 8. Polymeric hump]. CGSd: Corn starch-grape seed tannin complex, CGSk: Corn starch-grape skin tannin complex, PGSd: Pea starch-grape seed tannin complex, PGSk: Pea starch-grape skin tannin complex, WGSd: Wheat starch-grape seed tannin complex, WGSk: Wheat starch-grape skin tannin complex, GSd: Grape seed tannins, and GSk: Grape skin tannins.

of proanthocyanidins. This suggests that tannins were embedded in the amylose helix to develop inclusion complexes and as a result, hindered the insertion of iodine within the helical structure of amylose by making the exteriorly located hydroxyl groups unavailable, hence, decreasing the absorption (Alcázar-Alay & Meireles, 2015). The maximum absorbance peak observed for pea starch-tannin represented the proportion of starch chain length bound to the tannin molecules. Addition of tannins to pea starch-tannin complexes notably reduced the absorbance, indicating the incorporation of tannin molecules into the starch's helical cavity through the establishment of hydrophobic interactions, which blocked the binding sites for iodine to complex with starch. Higher cooking temperatures might have caused the expansion of starch molecular networks, enabling the tannins to enter inside the granular structure and helical cavity of amylose, which resulted in preventing the interaction of iodine with amylose chains, which led to a drop in the absorbance values for pea starch (Youming et al., 2024). For corn starch, it could be assumed that the tannins were bound to amylose chains by forming non-inclusion complexes between the two helices without changing the original crystalline type of the corn starch (Wu et al., 2024). The helical structure of amylose and the hydroxyl groups present at the exterior sites were still accessible to iodine and as a result the absorbance values remained unchanged for corn starch even after addition of tannins (Alcázar-Alay & Meireles, 2015; Youming et al., 2024). For wheat starch and their respective complexes, a significant change in the absorbance values of starch-tannin complexes signifies that either the iodine developed a direct interaction with amylose chain and got embedded within the hydrophobic core or the tannins developed non-inclusion complexes with starch but obstructed the iodine interaction with amylose helix and thus, explains the change in absorbance for wheat starch-tannin complexes (Amoako & Awika, 2019). Moreover, differences in the amylose content, presence of other biomolecules such as tannins and type of intermolecular interaction (hydrophobic and/or hydrophilic) can affect the conjugation of iodine to starch molecules (Alcázar-Alay & Meireles, 2015; Youming et al., 2024). The particle size for wheat starch-tannin complexes supported the formation non-inclusion complexes as the particle size of wheat starch remained unchanged after tannin addition, which suggests that tannins formed non-inclusion complexes with starch. However, the presence of tannins in the starch matrix restricted the insertion of iodine in the amylose helix but disrupted the colour development and decreased the absorbance values of the amylose-iodine complexes (Fig. 4I and J).

3.5. FTIR

Changes in the short range-ordered structure between different starches and starch-tannin complexes were investigated through FTIR studies (Fig. 4D–F). No new distinctive peaks emerged in the spectra, indicating that the starch and tannin molecules interacted exclusively via non-covalent bonding. In all three starches and starch-tannin complexes, a broad band in between 3423 and 3449 cm^{-1} was observed, which could be attributed to the –OH group stretching vibrations. An absorption maxima around 2929 cm^{-1} appeared due to the bending vibrations of the –OH group. Asymmetrical stretching vibrations of $–CH_2$ bond exhibited a distinctive peak closer to 1630-1640 cm^{-1}, an absorbance peak was found at 1465 cm^{-1}, which could be indicative of bending vibrations due to –CH bond. A broad band in between 900 and 1190 cm^{-1} was ascribed to the stretching vibration of C–O bond. The peak intensities for starch-tannin complexes shifted in contrast to starch samples upon complexation, confirming the interaction of tannins with starch via both hydrophobic interactions and hydrogen bonding (Liu et al., 2023; Youming et al., 2024).

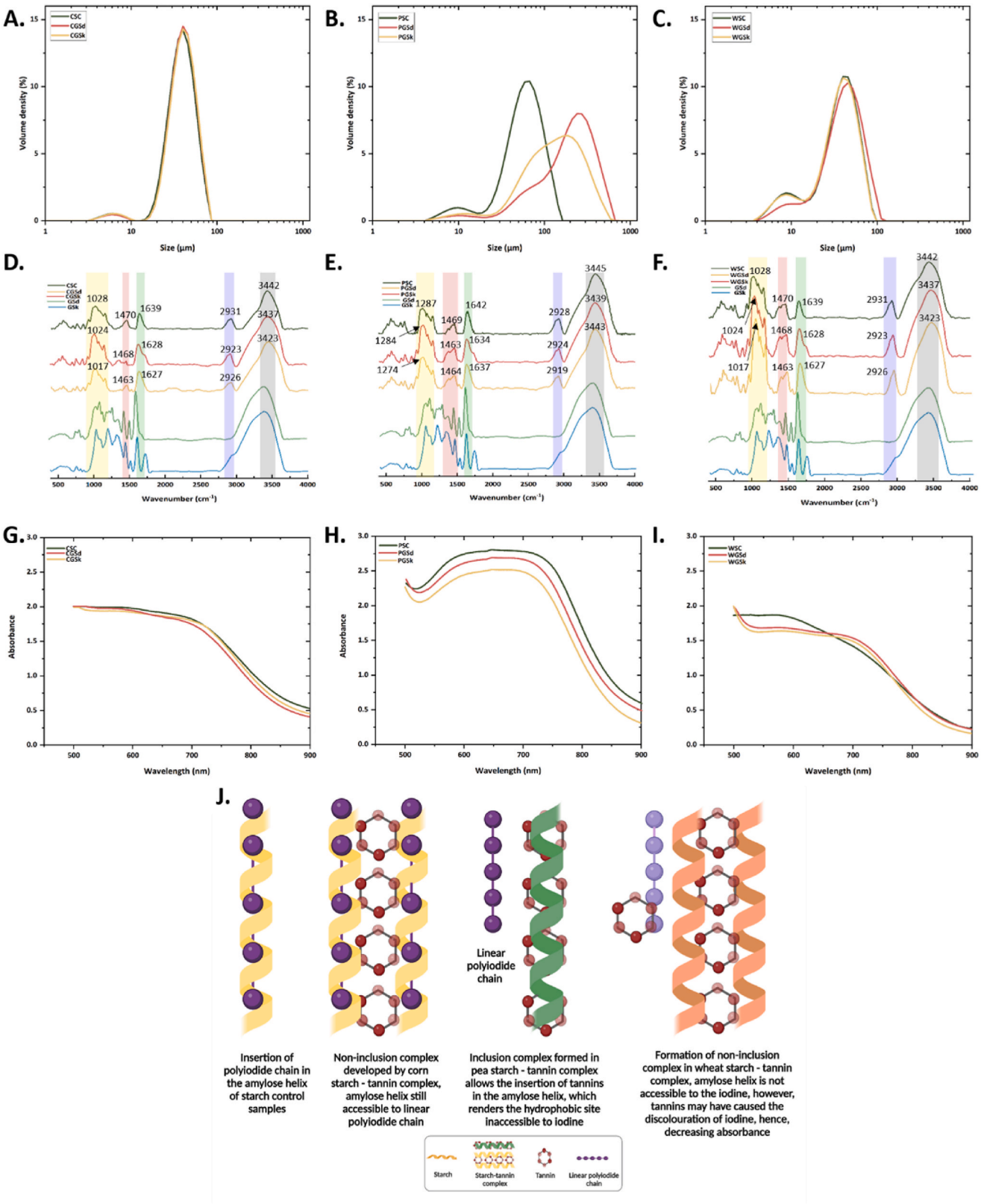

Fig. 4. Effect of GSd and GSk on the particle size distribution (A–C), FTIR spectra (D–F) and starch-iodine binding (G–I) of three different starches. (A, D, G) corn starch and its complexes, (B, E, H) pea starch and its complexes, and (C, F, I) wheat starch and its complexes, (J) Possible interactions of polyiodide chain with amylose helix and tannins in starch-tannin complexes. CSC: Corn starch control, CGSd: Corn starch-grape seed tannin complex, CGSk: Corn starch-grape skin tannin complex, PSC: Pea starch control, PGSd: Pea starch-grape seed tannin complex, PGSk: Pea starch-grape skin tannin complex, WSC: Wheat starch control, WGSd: Wheat starch-grape seed tannin complex, WGSk: Wheat starch-grape skin tannin complex, GSd: Grape seed tannins, GSk: Grape skin tannins.

Table 4
Back extrusion textural properties and power law model parameters determined by frequency sweep test for starch control samples and starch-tannin complexes. Power law model was used for frequency sweep tests of starch-tannin complexes (G' > G″), where parameters n', n", K', K" represents the slope and power-law model constants.

	Firmness (N)	Consistency (N.s)	Cohesiveness (N)	Index of viscosity (N.s)
CSC	0.75 ± 0.15^{bc}	18.17 ± 2.69^{bc}	-0.68 ± 0.14^{bc}	-1.61 ± 0.32^{ef}
CGSd	0.33 ± 0.01^{cd}	8.30 ± 0.33^{de}	-0.24 ± 0.01^{a}	-0.50 ± 0.04^{bc}
CGSk	0.54 ± 0.05^{bcd}	14.29 ± 0.96^{cd}	-0.51 ± 0.04^{b}	-1.21 ± 0.11^{de}
PSC	2.21 ± 0.41^{a}	36.01 ± 5.76^{a}	-1.39 ± 0.14^{d}	-2.09 ± 0.10^{g}
PGSd	0.24 ± 0.00^{b}	5.00 ± 0.22^{e}	-0.15 ± 0.01^{a}	-0.02 ± 0.00^{a}
PGSk	0.91 ± 0.10^{d}	16.45 ± 0.39^{bc}	-0.52 ± 0.07^{b}	-0.90 ± 0.01^{cd}
WSC	0.28 ± 0.04^{d}	6.14 ± 0.37^{e}	-0.18 ± 0.01^{a}	-0.22 ± 0.06^{ab}
WGSd	0.86 ± 0.03^{bc}	22.97 ± 0.77^{b}	-0.91 ± 0.02^{c}	-2.10 ± 0.05^{g}
WGSk	0.71 ± 0.07^{b}	19.38 ± 2.32^{bc}	-0.73 ± 0.12^{bc}	-1.74 ± 0.21^{fg}

	Flow point		
	γ (s^{-1})	**G' (Pa)**	**G" (Pa)**
CSC	0.101	7.92 ± 4.13^{c}	7.52 ± 3.72^{b}
CGSd	0.217	11.26 ± 2.70^{c}	11.75 ± 3.37^{b}
CGSk	0.217	24.96 ± 8.34^{bc}	27.08 ± 6.42^{b}
PSC	0.466	42.47 ± 25.46^{bc}	39.07 ± 11.95^{b}
PGSd	1.010	133.35 ± 57.77^{ab}	154.68 ± 55.84^{a}
PGSk	0.685	195.01 ± 80.96^{a}	161.08 ± 58.28^{a}
WSC	0.0685	0.73 ± 0.60^{c}	0.60 ± 0.46^{b}
WGSd	0.318	4.63 ± 1.58^{c}	5.41 ± 1.72^{b}
WGSk	0.466	4.56 ± 2.84^{c}	4.96 ± 1.91^{b}

Power law model parameters

	G' (Pa)			G" (Pa)		
	K' (Pa.s^{n})	n'	R^2	K" (Pa.s^{n})	n"	R^2
CSC	107.74 ± 2.15^{d}	0.04 ± 0.00^{b}	0.95 ± 0.01	2.74 ± 0.01^{e}	0.40 ± 0.00^{b}	0.98 ± 0.00
CGSd	161.44 ± 4.09^{c}	0.04 ± 0.00^{b}	0.97 ± 0.01	4.90 ± 0.08^{d}	0.35 ± 0.01^{cd}	0.99 ± 0.00
CGSk	196.49 ± 2.14^{b}	0.04 ± 0.00^{b}	0.97 ± 0.01	6.53 ± 0.16^{c}	0.34 ± 0.00^{d}	0.99 ± 0.00
PSC	153.47 ± 1.22^{c}	0.09 ± 0.00^{b}	0.99 ± 0.00	18.14 ± 0.06^{b}	0.07 ± 0.00^{e}	0.92 ± 0.00
PGSd	365.60 ± 8.70^{a}	0.07 ± 0.00^{b}	0.99 ± 0.00	36.48 ± 0.40^{a}	0.06 ± 0.00^{e}	0.92 ± 0.01
PGSk	14.52 ± 4.02^{g}	0.09 ± 0.03^{b}	0.96 ± 0.04	1.73 ± 0.37^{f}	0.10 ± 0.02^{e}	0.88 ± 0.05
WSC	0.71 ± 0.01^{g}	0.20 ± 0.04^{a}	0.94 ± 0.04	0.11 ± 0.01^{g}	0.58 ± 0.01^{a}	0.96 ± 0.03
WGSd	74.61 ± 5.17^{e}	0.08 ± 0.00^{b}	0.99 ± 0.01	4.95 ± 0.19^{d}	0.33 ± 0.02^{d}	0.99 ± 0.00
WGSk	44.38 ± 4.36^{f}	0.08 ± 0.01^{b}	0.98 ± 0.01	3.00 ± 0.47^{e}	0.39 ± 0.02^{bc}	0.99 ± 0.00

Data presented as mean ± standard deviation, same letters indicate treatments are not significantly different ($p < 0.05$).
CSC: Corn starch control, CGSd: Corn starch-grape seed tannin complex, CGSk: Corn starch-grape skin tannin complex, PSC: Pea starch control, PGSd: Pea starch-grape seed tannin complex, PGSk: Pea starch-grape skin tannin complex, WSC: Wheat starch control, WGSd: Wheat starch-grape seed tannin complex, WGSk: Wheat starch-grape skin tannin complex.

3.6. Textural properties

The back extrusion test of three different starches and their complexes with tannins revealed four different parameters: firmness, consistency, cohesiveness and index of viscosity (Table 4). Addition of GSd and GSk tannins to the starches significantly affected these textural properties. In case of both corn starch and pea starch, a significant drop in these textural properties was noted upon addition of tannins, suggesting a softer texture and less rigidity of these starch-tannin complexes when compared with corn (CSC) and pea starch (PSC) controls. In contrast to control samples, corn and pea starches treated with GSd and GSk tannins exhibited significant differences in the firmness values. This suggests that the sources of tannins (grape skin and seeds), as well as their structural characteristics, such as the degree of polymerization, monomeric and polymeric content, the number of hydroxyl groups, and the proportion of different tannin constituents (e.g., gallic acid, catechins, and epicatechins), can significantly influence starch retrogradation and recrystallization during storage (Wang et al., 2021; Wu et al., 2024; Xu et al., 2021).

For GSd tannins, the presence of both monomeric and polymeric tannins likely played a crucial role in modulating starch recrystallization. Their high density of external hydroxyl (—OH) groups may have enhanced moisture absorption, thereby reducing the availability of water molecules for interaction with starch. This likely inhibited the reassociation of starch chains into double helices, preventing the recovery of crystalline structures. The pronounced intermolecular interactions between tannins and starch, facilitated by hydrogen bonding and hydrophobic interactions (for corn and pea starches, as revealed by FTIR studies), appear to have taken precedence over intramolecular interactions within starch chains. Conversely, GSk tannins, as revealed by HPLC analysis, predominantly comprised monomeric tannins with fewer external hydroxyl groups compared to polymeric GSd tannins. This structural difference likely explains the variations in firmness observed between the same starch samples treated with GSd and GSk tannins. The reduced hydroxyl group availability in GSk tannins may have led to weaker interactions with starch molecules, resulting in distinct retorgradation and textural properties (Liu et al., 2023; Wang et al., 2021; Xu et al., 2021; Zhu et al., 2009). For corn and pea

starch-tannin complexes, the cohesiveness was significantly higher than in control samples, and the viscosity index also increased, indicating adhesion or improved bonding between tannins and starch molecules, as well as a thicker or more viscous texture.

Meanwhile, an opposite trend was observed for wheat starch, where the addition of tannins significantly increased the firmness and consistency compared to wheat starch control (WSC). However, a significant reduction in cohesiveness and viscosity index was noted in wheat starch upon tannin addition, suggesting reduced bonding and lesser viscosity, possibly due to retrogradation, gelling behavior, or insufficient tannins available to adequately bind with starch (Kumar et al., 2022; Kumar et al., 2018; Kumar, Brennan, Zheng, Kumar, & Brennan, 2024; Vernon-Carter et al., 2020).

Polyphenols can enhance the microstructure of starch in starch-based foods, significantly reducing hardness, but factors like polyphenol concentration and storage conditions also play a critical role (Wu et al., 2024). For wheat starch-tannin complexes, the concentration of tannins added to all the three starches was same, so it could be possible that the tannin concentration added to the wheat starch (0.05%) was very low, likely too minimal to have a profound effect on producing softer gels. This combined with the overnight storage of starch samples at 4 °C, may have led to moisture loss, resulting in increased firmness and consistency for wheat starch-grape seed tannin complex (WGSd) and wheat starch-grape skin tannin complex (WGSk) compared to WSC (Vernon-Carter et al., 2020).

For corn and pea starch-tannin complexes, both cohesiveness and index of viscosity had lower values than their control samples, potentially due to the interaction between the starch glycan chains and polyphenols, along with variations in starch retrogradation and viscosity parameters following tannin addition (Vernon-Carter et al., 2020). On the other hand, wheat starch-tannin complexes showed higher values for these textural properties than the wheat starch control, which may be attributed to the same factors affecting bonding, retrogradation and gelling behavior (Kumar et al., 2022; Kumar et al., 2018 Kumar, Brennan, Zheng, Kumar, & Brennan, 2024; Vernon-Carter et al., 2020). On the basis of these four extrusion parameters, valuable information can be collected to create food products that emphasize non-stickiness and flow ability.

3.7. Rheology

The dynamic rheological results of three different starches and starch-tannin complexes are presented in Fig. 5. The amplitude sweep results yielded two distinct regimes, the linear viscoelastic (LVE) regime and non-linear viscoelastic (NLVE) regime. The G′ and G" remained nearly unchanged in the LVE domain, while both G′ and G″ dropped in the NLVE range. For all the starches and starch-tannin complexes, the G′ was higher than G″ in the LVE region, however, the G′ decreased sharply, while for G″, it increased slightly before sharply decreasing after the crossover point in the NLVE range. Compared to the control samples, three different starches complexed with tannins showed a significant increase in G′ and G″ except for the PGSk complex (Fig. 5A–C). The values of G′ were higher than G″ for all starch-tannin complexes, which suggests that the elastic properties of starches were prominently being affected by the tannins (Xu et al., 2021). For all three starch control samples, the initial gap between G′ and G″ was smaller, meanwhile the addition of tannins increased the gap between G′ and G". For corn starch-grape seed tannin (CGSd) and corn-starch grape skin tannin (CGSk) complexes, the gap increased by 47% and 71%, for both PGSd and PGSk, a 33% increase in the gap was noticed and for WGSd and WGSk samples, the percent increase of 4–8% was observed (Fig. 5A–C). An increase in the initial gap between G′ and G″ for starch-tannin complexes along with higher G′ and G″ indicates that both GSd and GSk tannins significantly improved the viscoelastic properties of starch after interacting with amylose chains via hydrogen bonds. Kan and co-workers (2022), also observed a shift in the G' and G" for wheat starch upon addition of tannic acid. This suggested that the increased gel strength of starch-tannin complexes could be attributed to tannins, which enhance cross-linking within the starch matrix through hydrogen bonding. This leads to the development of stronger three-dimensional starch gel network, thereby increasing both the viscoelastic modulus and elastic behavior of the starch gels (Fig. 6) (Kan et al., 2022; Xu et al., 2021).

A shift in the crossover (or flow) point for starch-tannin complexes was also observed. For the control samples, the flow point occurred at 0.101 strain (%) for CSC, 0.466 strain (%) for PSC and 0.069 strain (%) for WSC, indicating the onset of non-linear viscoelastic behavior at lower deformation. However, for all starch-tannin complexes, the crossover point shifted to a higher strain, which was 0.217 strain (%) for corn starch-tannin complexes, 1.01 strain (%) for PGSd, 0.685 strain (%) for PGSk, 0.466 strain (%) for WGSd and 0.318 strain (%) for WGSk, respectively (Table 4). This shift to the right indicates that addition of tannins increased the resistance of starch gels to deformation, suggesting an improvement in the structural integrity of starch, which allowed it to withstand higher strain (Xu et al., 2021).

For frequency sweep, the storage modulus (G′) was greater than the loss modulus (G″), without any overlaps, suggesting that both starch-tannin complexes and control samples were displaying weak gel like behavior. The G′ and G″ increased after addition of tannins to the corn and wheat starch. However, in case of pea starch, the G′ and G″ remained unchanged after addition of GSd tannins, while it dropped in case of pea starch grape skin complexes (PGSk), prepared under the same cooking conditions (Fig. 5D–F). The initial gap between G′ and G″ also increased for all the starches after complexation with tannins except for the PGSk complex (Fig. 5D–F). Kan et al. (2022) obtained similar results and proposed that non-inclusion complexes formed in sufficient proportions contributed to the increased G′ and G″ in starch gels. These complexes acted as cross-links and were majorly responsible for the elastic behavior of the starch gels. However, in case of PGSk, an opposite trend was observed in contrast to PSC. It suggests that the tannins got embedded in the helical cavity of amylose upon complexation to form inclusion complexes by disrupting the entanglement of amylose chains and preventing the formation of the original helical structure which led to a decrease in G′ and G″ for PGSk (Kan et al., 2022; Youming et al., 2024). Moreover, these differences in G′ and G″ also suggest that the botanical source and composition of starch could equally influence the rheological properties of starch-tannin complexes despite the similar cooking conditions and tannin concentrations for the three starch-tannin complexes (Wu et al., 2024). The frequency sweep data with G' > G″ was fitted using power law model, presented in Table 4. Starches complexed with grape tannins showed different results than the control starch samples for the K and n parameters. Except for PGSk complex, addition of grape tannins to all other starches significantly increased the K′ values. A similar trend was observed for K″ values, which increased after complexation with tannins except for PGSk and WGSk complexes. On the other hand, the n' values dropped significantly for PGSd, WGSd and WGSk complexes and a reduction in the n" values was observed for CGSk, WGSd and WGSk complexes, while for other starches and their respective complexes, both n' and n" remained unchanged. A drop in the n values for WGSd and WGSk complexes signifies that in the presence of tannins, wheat starches developed a rigid gel network structure (Kan et al., 2022).

3.8. Antioxidant activity

The antioxidant capacity of starch-tannin complexes was determined in order to examine the ability of tannins to exhibit antioxidant properties upon complexation with starch. FRAP method was utilized to measure the capacity of GSd and GSk tannins complexed with starch molecules to compete for peroxyl radical. The results of radical scavenging capacity of three different starch control and starch–grape tannin complexes are presented in Fig. 7A. The antioxidant activity of all three

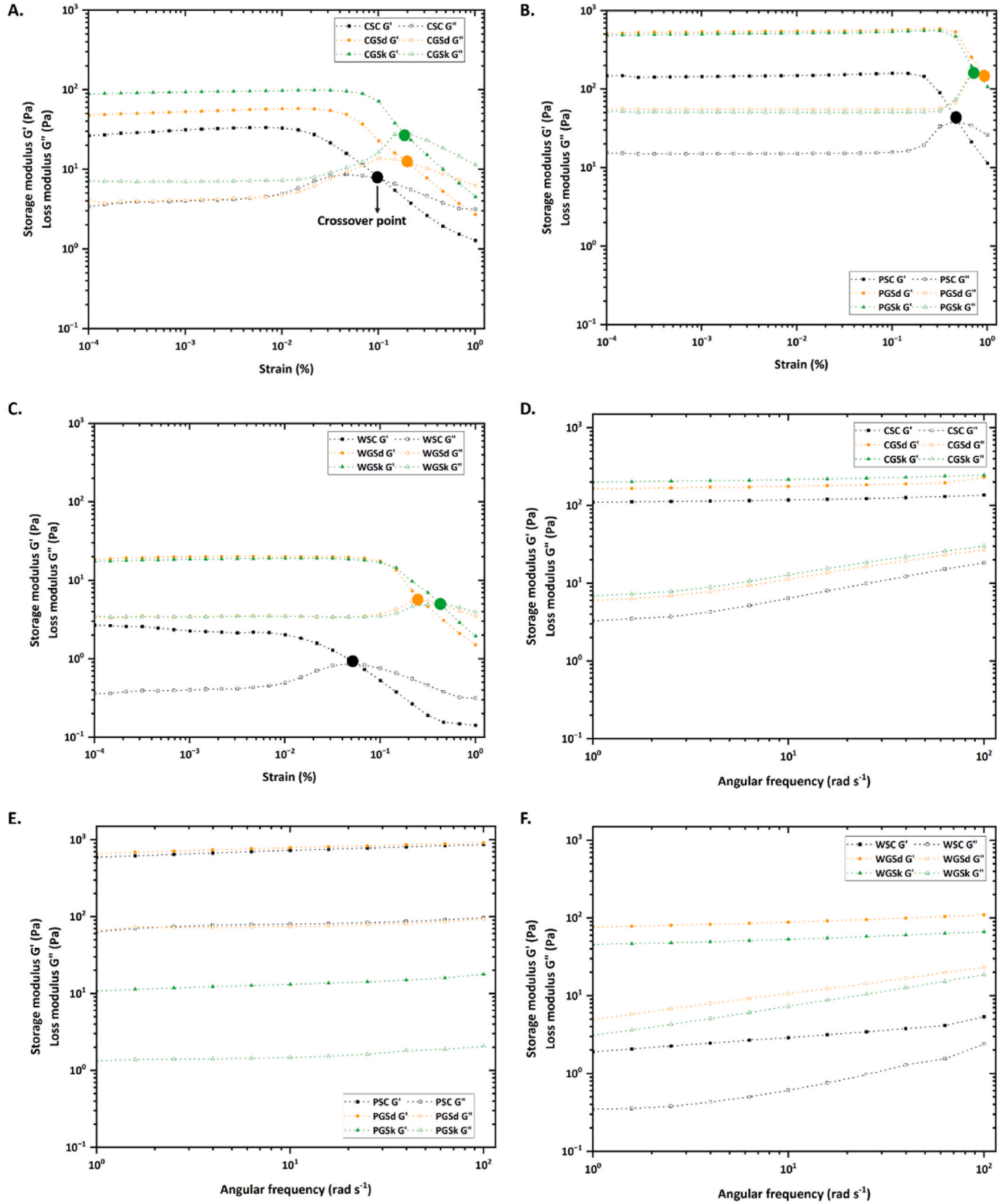

Fig. 5. The trend in the change of storage modulus (G′) and loss modulus (G″) with amplitude and frequency for three different starches and their respective starch-tannin complexes. Amplitude sweep test of (A) corn starch and its complexes, (B) pea starch and its complexes, and (C) wheat starch and its complexes, and frequency sweep test of (D) corn starch and its complexes, (E) pea starch and its complexes, and (F) wheat starch and its complexes. CSC: Corn starch control, CGSd: Corn starch-grape seed tannin complex, CGSk: Corn starch-grape skin tannin complex, PSC: Pea starch control, PGSd: Pea starch-grape seed tannin complex, PGSk: Pea starch-grape skin tannin complex, WSC: Wheat starch control, WGSd: Wheat starch-grape seed tannin complex, WGSk: Wheat starch-grape skin tannin complex.

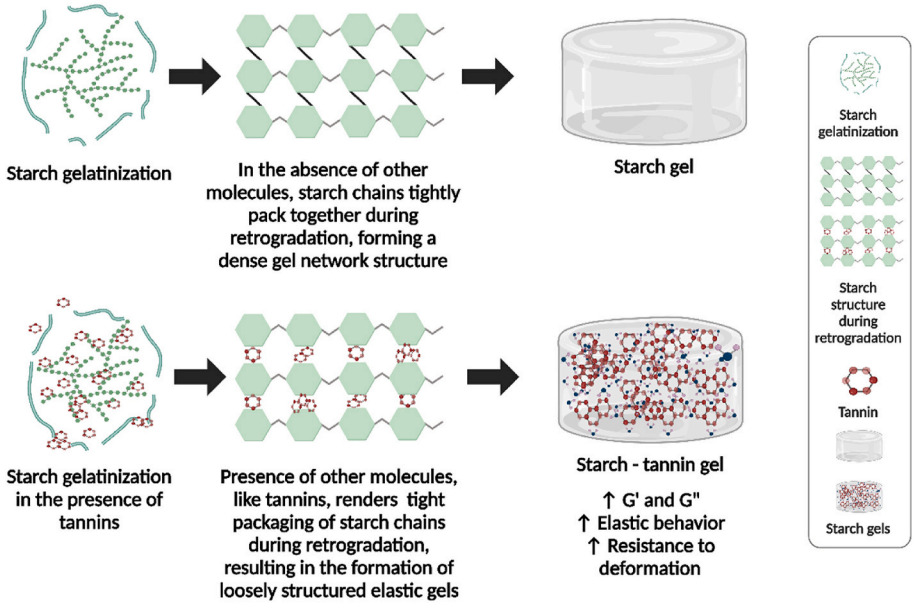

Fig. 6. Schematic representation of effect of tannins on the rheological properties of starch.

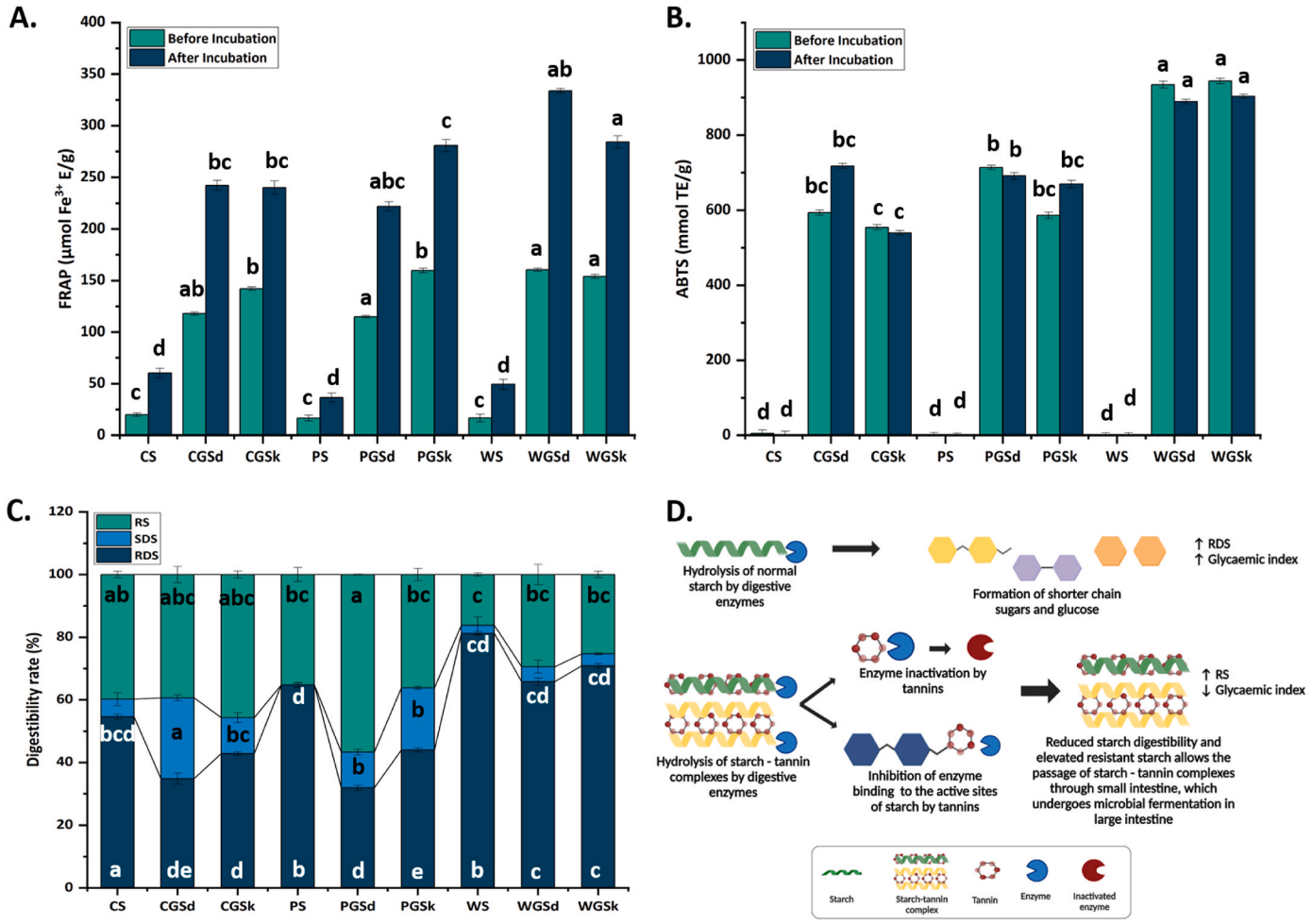

Fig. 7. Effect of tannin interaction on the antioxidant activity (A) FRAP, (B) ABTS, (C) RDS, SDS and RS of three different starch-tannin complexes, and (D) Proposed mechanism for starch digestion regulation by tannins in starch-tannin complexes. CSC: Corn starch control, CGSd: Corn starch-grape seed tannin complex, CGSk: Corn starch-grape skin tannin complex, PSC: Pea starch control, PGSd: Pea starch-grape seed tannin complex, PGSk: Pea starch-grape skin tannin complex, WSC: Wheat starch control, WGSd: Wheat starch-grape seed tannin complex, WGSk: Wheat starch-grape skin tannin complex. Statistically significant differences between the values of samples prior to incubation and after 4 h of incubation are represented by different alphabetical letters ($p < 0.05$).

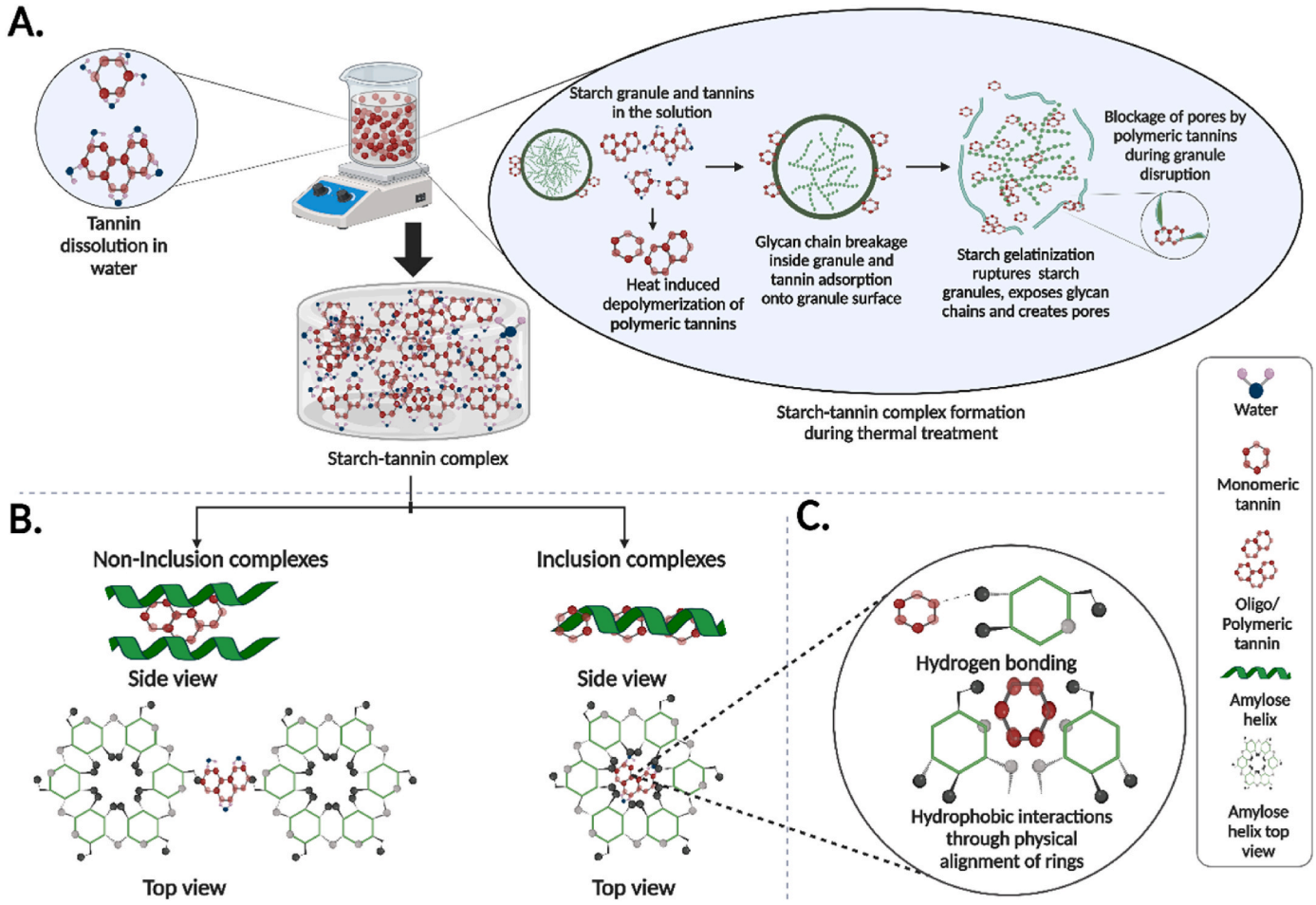

Fig. 8. Proposed mechanism of the possible interactions between starch molecules and grape tannins. (A) During thermal treatment, starch gelatinizes, leading to granule rupture, exposure of glycan chains and pore formation, facilitating subsequent interactions with tannin molecules, (B) Tannins associate with glycan chains through two primary mechanisms: hydrophilic interactions and hydrogen bonding, forming non-inclusion complexes or hydrophobic interactions, where tannins insert into amylose helices to form inclusion complexes, and (C) Hydrogen bonding primarily involves hydroxyl (-OH) groups on starch and tannin molecules, while hydrophobic interactions occur between the aromatic rings of tannins and the hydrophobic domains of amylose chains, stabilizing the complexes.

different starch-tannin complexes was higher than that of the starch control samples. While, prior to the 4 h incubation, the starch–grape skin tannin complexes exhibited the highest antioxidant capacity, which was 141.97 μmol Fe^{3+} E/g sample for CGSk, 159.73 μmol Fe^{3+} E/g sample for PGSk and 153.96 μmol Fe^{3+} E/g sample for WGSk, respectively. For starch–grape seed tannin complexes, the antioxidant capacity ranged from 114.98 μmol Fe^{3+} E/g sample to 160.50 μmol Fe^{3+} E/g sample. After 4 h of incubation, the antioxidant capacity for all the starch–grape tannin complexes showed a significant increase ranging from 221 μmol Fe^{3+} E/g sample to 333 μmol Fe^{3+} E/g sample.

The scavenging activities of starch control samples were significantly lower than the antioxidant capacity of starch-tannin complexes samples, which ranged from 16 to 19 μmol Fe^{3+} E/g sample before incubation. Even after 4 h of incubation, the control samples exhibited the weakest FRAP values, ranging from 36 to 60 μmol Fe^{3+} E/g sample.

A similar trend of antioxidant activities was observed for starch control and starch-tannin complexes through ABTS antioxidant assay, where wheat starches complexed with grape tannins exhibited the highest antioxidant activity (Fig. 7B).

Phenolic acids possess antioxidant activity as these compounds can donate electrons or hydrogen to other molecules to create stable radical intermediates. This process can prevent or delay the oxidation of food products. Grape tannins are rich in phenolic compounds and exhibit both anti-oxidative and radical scavenging abilities. Thermal treatment of starch-tannin complexes at higher temperatures might have aided in the conversion of insoluble phenolic compounds to their solubilized form, which could be associated with increased antioxidant activity and reducing power. Moreover, greater the quantity of phenolic content in the sample, higher is its antioxidant capacity (Kim et al., 2006). HPLC studies revealed that the proportion of tannins (catechin and epicatechin) bound to starch was greater, suggesting a correlation between phenolic content and antioxidant activity (data shown in Table 3). Thus, it can be concluded that tannins after complexation with starch molecules were capable of exhibiting antioxidant properties, which can aid in enhancing the nutritional properties of food containing starch (Kim et al., 2006; Wu et al., 2021). Youming et al. (2024) observed an increase in the antioxidant activity of corn starch upon complexation with tannic acid. Tannins exhibit antioxidant properties and cooking of starch at higher temperatures was found to escalate molecular interaction with tannins, which resulted in elevated overall antioxidant capacity-cum-nutritional profile of starch-tannic acid complex.

3.9. *In-vitro starch digestibility*

GSd and GSk tannins decreased the rapidly digesting starch (RDS) for all the three starches significantly, while increased the slowly digesting starch (SDS) and resistant starch (RS) for pea and wheat starches significantly ($p < 0.05$). For untreated starches, RDS was significantly higher, 46.53 % (CSC), 39.72 % (PSC) and 38.79 % (WSC), which decreased significantly upon tannin addition. For complexes formed

using GSk, RDS decreased to 27.51% (CGSk), 23.43 % (PGSk) and 34.54 % (WGSk). In case of starch-grape seed tannin complexes, RDS decreased to 24.74 % (CGSd), 27.48 % (PGSd) and 33.41 % (WGSd). The SDS for CSC, CGSk and CGSd was 4.81 %, 7.38 % and 18.33 %; for PSC, PGSk and PGSd, it was 0 %, 10.57 % and 9.76 %; and for WSC, WGSk and WGSd, it was 1.22 %, 1.89 % and 2.43 %, respectively. The decrease in starch digestibility indicates the prominent influence and capability of tannins to hinder the digestibility of respective starches. The RS content for starch-tannin complexes prominently increased under the influence of tannins, with PGSd and wheat starch-tannin complexes exhibiting significant increase in RS content, which increased by 19% for the former complex and by 5–7% in the latter complex as compared to their respective control starch samples (Fig. 7C). This suggests that tannins could form slow-digesting and/or non-digestible complexes with starch, which can prevent starch digestion effectively and the inhibition impact can be largely determined by the starch amylose content and tannin content (Wu et al., 2024; Youming et al., 2024). The tannins may have either embedded within the helical structure of glycan chains or between two glycan chains, thereby altering or shielding the attacking sites from digesting enzymes during complexation process, which makes tannins capable of inhibiting the enzyme activity and preventing its interaction with starch, thereby reducing starch digestion rates (Youming et al., 2024; Zhang et al., 2023). It could be assumed that tannins might associate with the amino acid residues of starch digesting enzymes through hydrophobic interactions and as a result might impede enzymes ability to digest starch. Starch properties such as swelling power can also prevent the enzyme interaction with starch molecules. Presence of tannins can alter the structure of starch granules by blocking the hydroxyl groups in starch through non-covalent interactions. As a result, this can allow the passage of starch through small intestine without being digested, leading to its eventual fermentation by microbes in the large intestine (Chou et al., 2020; Kan et al., 2022; Xu et al., 2021). Youming et al. (2024) prepared corn starch–tannic acid at different temperatures ranging from 25 to 95 °C and reported a decrease in RDS and SDS. They concluded that tannins can inhibit the activity of digestive enzymes such as α-amyloglucosidase and α-amylase by adhering to gelatinized starch molecules, which can restrict the exposure of catalytic sites on starch to digestive enzymes, leading to a delay in starch hydrolysis (Fig. 7D). Based on this, healthy starch foods imparting lower glycemic index can be prepared.

3.10. Proposed possible interactions between starch and tannins

Cooking of starch at high temperatures causes its gelatinization, which ruptures the starch granules, creates pores and exposes the amylose and amylopectin chains. Tannins, present in the matrix, start interacting with starch. Polymeric tannins may adsorb onto the pores of starch granules, while monomeric/oligomeric tannins can enter inside the granule through the pores formed after the granules rupture (Fig. 8A). These tannins can further incorporate into the helical structure of starch molecules, altering the crystalline structure of starch. Tannins may also bind to the surface of starch granules via various molecular interactions or form inclusion or non-inclusion complexes (Ngo et al., 2022; Rostamabadi et al., 2023; Youming et al., 2024). Based on the particle size, starch-iodine binding and FTIR studies, we tried to illustrate the interaction of grape tannins with starches derived from three different botanical sources. In case of pea starch-tannin complexes, an increase in the particle size of starch, a decrease in the absorbance values during starch-iodine binding and a shift in the vibrations of different groups upon tannin complexation suggested the insertion of grape tannins within the helical structure of amylose via hydrophobic interactions, thus, leading to the formation of inclusion complexes. While for corn and wheat starches, no changes in the particle size, no or minimal decrease in absorbance values for starch-iodine complexes and a large shift in the spectral peaks for hydroxyl groups indicated the incorporation of tannins in between the two amylose chains through hydrophilic interactions and hydrogen bonding to form non-inclusion complexes while maintaining its inherent crystalline structure (Fig. 8B). Tannins can form stable complexes with starch through hydrogen bonding and other non-covalent interactions (hydrophilic and/or hydrophobic). In hydrogen bonding, tannins bind with the hydroxyl groups present on the starch molecules. Aromatic rings present in tannins contain hydrophobic regions, which repel water and associate with the hydrophobic entities of starch (formed due to complex arrangement of glucose in starch granules), leading to hydrophobic molecular interactions. The two biomolecules are in close proximity when bound to each other through hydrophobic interactions, thus, forming stable starch-tannin complexes (Fig. 8C) (Zhu, 2010, 2015).

4. Conclusion

Starch, a crucial macro nutrient, is present in all food types and varies in concentration, structural and physicochemical properties from one source to other. Its ability to interact with other biomolecules present in the food matrix alters its textural-cum nutritional profile predominantly. This study showed an effective binding of monomeric/oligomeric GSk and condensed GSd tannins with starch upon complexation at higher temperatures. Physicochemical changes in starch upon tannin addition revealed the formation of inclusion complexes in pea starch and non-inclusion complexes in corn and wheat starches. Wheat starches produced firmer gels analyzed through textural studies. Starch-tannin gels with enhanced elastic behavior were formed as revealed by increased storage modulus (G') and loss modulus (G") of freshly prepared gels. Tannins significantly increased the antioxidant properties of starches and reduced in-vitro starch digestibility. A significant increase in resistant starch (RS) content, specifically in pea starch–grape seed tannin (PGSd) complex and a decrease in rapidly digestible starch (RDS) for all the three starches was noticed. These findings can aid in the selection of starches from different botanical sources for complexation with tannins to develop the foods with desired physicochemical and rheological properties along with improved digestibility. Furthermore, this knowledge can provide valuable insights for the food industry in selecting appropriate starches based on tannin influences, paving the way for future research on starch-tannin interactions and their health benefits, such as lowering glycemic response through in-vivo studies.

CRediT authorship contribution statement

Harkamal Kaur: Writing – review & editing, Writing – original draft, Visualization, Software, Methodology, Investigation, Formal analysis, Data curation. **Annu Mehta:** Writing – review & editing, Methodology. **Lokesh Kumar:** Writing – review & editing, Writing – original draft, Validation, Supervision, Resources, Project administration, Methodology, Investigation, Funding acquisition, Conceptualization.

Declaration of competing interest

The authors declare that they have no known competing financial interests or personal relationships that could have appeared to influence the work reported in this paper.

Acknowledgements

We are thankful to Richard Hider and Rosy Tung for their invaluable assistance with the MCP, HPLC and mDP experiments conducted in this study. We would like to acknowledge Lincoln University faculty research fund to support the experimental cost.

Data availability

Data will be made available on request.

References

Alcázar-Alay, S. C., & Meireles, M. A. A. (2015). Physicochemical properties, modifications and applications of starches from different botanical sources. *Food Science and Technology, 35*, 215–236.

Amoako, D., & Awika, J. M. (2016a). Polyphenol interaction with food carbohydrates and consequences on availability of dietary glucose. *Current Opinion in Food Science, 8*, 14–18.

Amoako, D. B., & Awika, J. M. (2016b). Polymeric tannins significantly alter properties and in vitro digestibility of partially gelatinized intact starch granule. *Food Chemistry, 208*, 10–17.

Amoako, D. B., & Awika, J. M. (2019). Resistant starch formation through intrahelical V-complexes between polymeric proanthocyanidins and amylose. *Food Chemistry, 285*, 326–333.

Apriyanto, A., Compart, J., & Fettke, J. (2022). A review of starch, a unique biopolymer–Structure, metabolism and in planta modifications. *Plant Science, 318*, Article 111223.

Barrett, A. H., Farhadi, N. F., & Smith, T. J. (2018). Slowing starch digestion and inhibiting digestive enzyme activity using plant flavanols/tannins—a review of efficacy and mechanisms. *LWT, 87*, 394–399.

Barros, F., Awika, J. M., & Rooney, L. W. (2012). Interaction of tannins and other sorghum phenolic compounds with starch and effects on in vitro starch digestibility. *Journal of Agricultural and Food Chemistry, 60*(46), 11609–11617.

Bridson, J. H., Al-Hakkak, F., Steward, D., & Al-Hakkak, J. (2019). Preparation and morphological, rheological, and structural characterisation of proanthocyanidin coated starch granules. *Industrial Crops and Products, 130*, 285–291.

Butt, M. S., Sultan, M. T., Aziz, M., Naz, A., Ahmed, W., Kumar, N., & Imran, M. (2015). Persimmon (Diospyros kaki) fruit: Hidden phytochemicals and health claims. *EXCLI journal, 14*, 542.

Chen, W., Chiu, H. T., Feng, Z., Maes, E., & Serventi, L. (2021). Effect of spray-drying and freeze-drying on the composition, physical properties, and sensory quality of pea processing water (Liluva). *Foods, 10*(6), 1401.

Chou, S., Li, B., Tan, H., Zhang, W., Zang, Z., Cui, H., Wang, H., Zhang, S., & Meng, X. (2020). The effect of pH on the chemical and structural interactions between apple polyphenol and starch derived from rice and maize. *Food Science and Nutrition, 8*(9), 5026–5035.

Compart, J., Singh, A., Fettke, J., & Apriyanto, A. (2023). Customizing starch properties: A review of starch modifications and their applications. *Polymers, 15*(16), 3491.

de Morais Cardoso, L., Pinheiro, S. S., Martino, H. S. D., & Pinheiro-Sant'Ana, H. M. (2017). Sorghum (Sorghum bicolor L.): Nutrients, bioactive compounds, and potential impact on human health. *Critical Reviews in Food Science and Nutrition, 57*(2), 372–390.

Donmez, D., Pinho, L., Patel, B., Desam, P., & Campanella, O. H. (2021). Characterization of starch–water interactions and their effects on two key functional properties: Starch gelatinization and retrogradation. *Current Opinion in Food Science, 39*, 103–109.

Du, J., Yao, F., Zhang, M., Khalifa, I., Li, K., & Li, C. (2019). Effect of persimmon tannin on the physicochemical properties of maize starch with different amylose/amylopectin ratios. *International Journal of Biological Macromolecules, 132*, 1193–1199.

Esfandi, R., Willmore, W. G., & Tsopmo, A. (2019). Peptidomic analysis of hydrolyzed oat bran proteins, and their in vitro antioxidant and metal chelating properties. *Food Chemistry, 279*, 49–57.

Gu, H.-F., Li, C.-M., Xu, Y.-j., Hu, W.-f., Chen, M.-h., & Wan, Q.-h. (2008). Structural features and antioxidant activity of tannin from persimmon pulp. *Food Research International, 41*(2), 208–217.

Gutierrez, A. S. A., Guo, J., Feng, J., Tan, L., & Kong, L. (2020). Inhibition of starch digestion by gallic acid and alkyl gallates. *Food Hydrocolloids, 102*, Article 105603.

Hernández, H. A. R., Gutiérrez, T. J., & Bello-Pérez, L. A. (2022). Can starch-polyphenol V-type complexes be considered as resistant starch? *Food Hydrocolloids, 124*, Article 107226.

Jane, J.-l. (2004). Starch: Structure and properties. *Chemical and functional properties of food saccharides*, 81–101.

Kan, L., Capuano, E., Oliviero, T., & Renzetti, S. (2022). Wheat starch-tannic acid complexes modulate physicochemical and rheological properties of wheat starch and its digestibility. *Food Hydrocolloids, 126*, Article 107459.

Kennedy, J. A., Hayasaka, Y., Vidal, S., Waters, E. J., & Jones, G. P. (2001). Composition of grape skin proanthocyanidins at different stages of berry development. *Journal of Agricultural and Food Chemistry, 49*(11), 5348–5355.

Kennedy, J. A., & Jones, G. P. (2001). Analysis of proanthocyanidin cleavage products following acid-catalysis in the presence of excess phloroglucinol. *Journal of Agricultural and Food Chemistry, 49*(4), 1740–1746.

Kim, S.-Y., Jeong, S.-M., Park, W.-P., Nam, K., Ahn, D., & Lee, S.-C. (2006). Effect of heating conditions of grape seeds on the antioxidant activity of grape seed extracts. *Food Chemistry, 97*(3), 472–479.

Kumar, L., Brennan, M., Brennan, C., & Zheng, H. (2022). Thermal, pasting and structural studies of oat starch-caseinate interactions. *Food Chemistry, 373*, Article 131433.

Kumar, L., Brennan, M., Zheng, H., & Brennan, C. (2018). The effects of dairy ingredients on the pasting, textural, rheological, freeze-thaw properties and swelling behaviour of oat starch. *Food Chemistry, 245*, 518–524.

Kumar, L., Brennan, M., Zheng, H., Kumar, G., & Brennan, C. (2024). Protein fortification in oat flour gel using various dairy protein ingredients: An evaluation of textural and pasting properties. *International Journal of Dairy Technology, 77*(1), 71–80.

Li, J., Shen, M., Xiao, W., Li, Y., Pan, W., & Xie, J. (2023). Regulating the physicochemical and structural properties of different starches by complexation with tea polyphenols. *Food Hydrocolloids, 142*, Article 108836.

Li, K., Yao, F., Du, J., Deng, X., & Li, C. (2018). Persimmon tannin decreased the glycemic response through decreasing the digestibility of starch and inhibiting α-amylase, α-glucosidase, and intestinal glucose uptake. *Journal of Agricultural and Food Chemistry, 66*(7), 1629–1637.

Liu, W., Xu, J., Shuai, X., Geng, Q., Guo, X., Chen, J., Li, T., Liu, C., & Dai, T. (2023). The interaction and physicochemical properties of the starch-polyphenol complex: Polymeric proanthocyanidins and maize starch with different amylose/amylopectin ratios. *International Journal of Biological Macromolecules, 253*, Article 126617.

Luo, D., Fan, J., Jin, M., Zhang, X., Wang, J., Rao, H., & Xue, W. (2024). The influence mechanism of pH and polyphenol structures on the formation, structure, and digestibility of pea starch-polyphenol complexes via high-pressure homogenization. *Food Research International, 114913*.

Luo, Y., Zhou, Y., Liu, H., Liu, X., Xie, X., & Li, L. (2024). Insight into the multi-scale structure and retrogradation of corn starch by partial gelatinization synergizing with epicatechin/epigallocatechin gallate. *Food Chemistry, 453*, Article 139568.

Miao, M., Jiang, H., Jiang, B., Zhang, T., Cui, S. W., & Jin, Z. (2014). Phytonutrients for controlling starch digestion: Evaluation of grape skin extract. *Food Chemistry, 145*, 205–211.

Mkandawire, N. L., Kaufman, R. C., Bean, S. R., Weller, C. L., Jackson, D. S., & Rose, D. J. (2013). Effects of sorghum (Sorghum bicolor (L.) Moench) tannins on α-amylase activity and in vitro digestibility of starch in raw and processed flours. *Journal of Agricultural and Food Chemistry, 61*(18), 4448–4454.

Mohamed, I. O. (2023). Interaction of starch with some food macromolecules during the extrusion process and its effect on modulating physicochemical and digestible properties. A review. *Carbohydrate Polymer Technologies and Applications*, Article 100294.

Ngo, T. V., Kusumawardani, S., Kunyanee, K., & Luangsakul, N. (2022). Polyphenol-modified starches and their applications in the food industry: Recent updates and future directions. *Foods, 11*(21), 3384.

Obadi, M., & Xu, B. (2021). Review on the physicochemical properties, modifications, and applications of starches and its common modified forms used in noodle products. *Food Hydrocolloids, 112*, Article 106286.

Prommajak, T., Leksawasdi, N., & Rattanapanone, N. (2020). Tannins in fruit juices and their removal. *Chiang Mai University Journal of Natural Sciences, 19*(1), 76–90.

Re, R., Pellegrini, N., Proteggente, A., Pannala, A., Yang, M., & Rice-Evans, C. (1999). Antioxidant activity applying an improved ABTS radical cation decolorization assay. *Free radical biology and medicine, 26*(9–10), 1231–1237.

Ribeiro de Barros, F. (2012). *Sorghum tannins: Interaction with starch and its effects on in vitro starch digestibility*.

Rostamabadi, H., Bajer, D., Demirkesen, I., Kumar, Y., Su, C., Wang, Y., Nowacka, M., Singha, P., & Falsafi, S. R. (2023). Starch modification through its combination with other molecules: Gums, mucilages, polyphenols and salts. *Carbohydrate Polymers, 120905*.

Salazar-Orbea, G. L., García-Villalba, R., Tomás-Barberán, F. A., & Sánchez-Siles, L. M. (2021). High–pressure processing vs. thermal treatment: Effect on the stability of polyphenols in strawberry and apple products. *Foods, 10*(12), 2919.

Smith, P. (2015). Measuring tannins in grapes and red wine using the MCP (methyl cellulose precipitable tannin assay). *T. A. W. R. Institute*.

Sochorova, L., Prusova, B., Cebova, M., Jurikova, T., Mlcek, J., Adamkova, A., Nedomova, S., Baron, M., & Sochor, J. (2020). Health effects of grape seed and skin extracts and their influence on biochemical markers. *Molecules, 25*(22), 5311.

Takahama, U., & Hirota, S. (2018). Interactions of flavonoids with α-amylase and starch slowing down its digestion. *Food & Function, 9*(2), 677–687.

Vernon-Carter, E., Alvarez-Ramirez, J., Bello-Perez, L., Gonzalez, M., Reyes, I., & Alvarez-Poblano, L. (2020). Supplementing white maize masa with anthocyanins: Effects on masa rheology and on the in vitro digestibility and hardness of tortillas. *Journal of Cereal Science, 91*, Article 102883.

Wang, C., An, X., Lu, Y., Li, Z., Gao, Z., & Tian, S. (2022). Biodegradable active packaging material containing grape seed ethanol extract and corn starch/κ-carrageenan composite film. *Polymers, 14*(22), 4857.

Wang, M., Chen, J., Chen, S., Ye, X., & Liu, D. (2021). Inhibition effect of three common proanthocyanidins from grape seeds, peanut skins and pine barks on maize starch retrogradation. *Carbohydrate Polymers, 252*, Article 117172.

Wang, R., Li, M., Brennan, M. A., Dhital, S., Kulasiri, D., Brennan, C. S., & Guo, B. (2023). Complexation of starch and phenolic compounds during food processing and impacts on the release of phenolic compounds. *Comprehensive Reviews in Food Science and Food Safety, 22*(4), 3185–3211.

Watrelot, A. A., & Norton, E. L. (2020). Chemistry and reactivity of tannins in vitis spp.: A review. *Molecules, 25*(9), 2110.

Wei, X., Li, J., & Li, B. (2019). Multiple steps and critical behaviors of the binding of tannic acid to wheat starch: Effect of the concentration of wheat starch and the mass ratio of tannic acid to wheat starch. *Food Hydrocolloids, 94*, 174–182.

Wu, G., Hui, X., Stipkovits, L., Rachman, A., Tu, J., Brennan, M. A., & Brennan, C. S. (2021). Whey protein-blackcurrant concentrate particles obtained by spray-drying and freeze-drying for delivering structural and health benefits of cookies. *Innovative Food Science & Emerging Technologies, 68*, Article 102606.

Wu, Y., Liu, Y., Jia, Y., Zhang, H., & Ren, F. (2024). Formation and application of starch–polyphenol complexes: Influencing factors and rapid screening based on chemometrics. *Foods, 13*(10), 1557.

Xu, J., Dai, T., Chen, J., He, X., Shuai, X., Liu, C., & Li, T. (2021). Effects of three types of polymeric proanthocyanidins on physicochemical and in vitro digestive properties of potato starch. *Foods, 10*(6), 1394.

Xu, T., Li, X., Ji, S., Zhong, Y., Simal-Gandara, J., Capanoglu, E., Xiao, J., & Lu, B. (2021). Starch modification with phenolics: Methods, physicochemical property alteration, and mechanisms of glycaemic control. *Trends in Food Science & Technology, 111*, 12–26.

Youming Zuo, F. Z., Jiang, S., Sui, Z., & Kong, X. (2024). Structural, physicochemical, and digestive properties of starch-tannic acid complexes modulated by co-heating temperatures. *Food Hydrocolloids, 109822*. https://doi.org/10.1016/j.foodhyd.2024.109822

Zhang, Q., Fan, S., Xie, H., Zhang, Y., & Fu, L. (2023). Polyphenols from pigmented quinoa as potential modulators of maize starch digestion: Role of the starch-polyphenol inclusion and non-inclusion complexes. *Food Hydrocolloids, 144*, Article 108975.

Zhang, Z., Tian, J., Fang, H., Zhang, H., Kong, X., Wu, D., Zheng, J., Liu, D., Ye, X., & Chen, S. (2020). Physicochemical and digestion properties of potato starch were modified by complexing with grape seed proanthocyanidins. *Molecules, 25*(5), 1123.

Zhu, F. (2010). *Interactions of carbohydrates with phenolic compounds*. HKU Theses Online (HKUTO).

Zhu, F. (2015). Interactions between starch and phenolic compound. *Trends in Food Science & Technology, 43*(2), 129–143.

Zhu, F., Cai, Y.-Z., Sun, M., & Corke, H. (2009). Effect of phytochemical extracts on the pasting, thermal, and gelling properties of wheat starch. *Food Chemistry, 112*(4), 919–923.